Generation of coherent far-infrared radiation using lasers

A. A. Vedenov, G. D. Myl'nikov, and D. N. Sobolenko

I. V. Kurchatov Institute of Atomic Energy, Academy of Sciences of the USSR, Moscow
Usp. Fiz. Nauk **138**, 477–515 (November 1982)

A review is given of methods used for generating coherent far-infrared radiation. They include the isolation of the frequency difference between two lasers, SRS by polaritons, optical pumping of gases, and the development of the electrical-discharge laser. Basic principles underlying the realization of the phenomena on which the above methods of generating far-infrared radiation are based are discussed. The properties of the working media, i.e., nonlinear properties of crystal converters (exploited in isolating the difference frequency and in SRS by polaritons) are described. Methods of producing inversion of level populations in gases used in lasers (pumped optically or by an electrical discharge) are analyzed. Specific schemes and device designs for the far infrared are described, and the possibilities and likely performance of these schemes are discussed. The review does not cover electron-beam generators (backward-wave tube, gyrotrons, etc.).

PACS numbers: 42.65.Cq, 42.80. – f, 42.72. + h, 42.55. – f

TABLE OF CONTENTS

1. INTRODUCTION

A review devoted to experimental techniques for the far infrared (wavelength $\lambda = 50–1000$ μm, $1/\lambda = 10–200$ cm^{-1}) was published in the 1969 volume of this journal.[1] Recent years have seen the development of new generators for this range (exploitation of beats between two infrared waves, polaritons, and resonant stimulated Raman scattering) with continuous or quasicontinuous (over a dense series of discrete lines) wavelength tuning. Generation has also been achieved in this range for hundreds of discrete lines due to molecular and atomic transitions under excitation by electrical discharge or optical pumping. Absorption, reflection, and nonlinear properties of many materials have been investigated in the far infrared, and new radiation detectors have been developed.

Table I lists some of the parameters of modern generators of far-infrared radiation, i.e., lasers or systems excited by lasers.

Generators of far-infrared radiation (FIR) can be used to investigate the physical properties of gases (rotational spectra of molecules,[3] spectra due to the internal rotation of radicals in complex molecules,[6,7] and so on), liquids,[4] solids (spectra of semiconductors[7], polymeric complexes[5]), and plasmas (diagnostics of large plasma installations for thermonuclear research[8,216]). The generators are also being successfully used to simulate microwave devices.[217,218] Images of objects illuminated by far-infrared radiation have been recorded.[2]

Powerful pulsed generators of infrared radiation of intermediate wavelength have been successfully used for collisionless multiphoton dissociation of certain

TABLE I.

	Pulse power, W	pulse length, s	Wavelength, μm	Continuous power, W
Wave mixing in solids	$1—10^3$	$10^{-8}—10^{-6}$	70—1000	10^{-6}
Polariton generator	10^2	10^{-8}	50—700	—
Optical pumping	$10^3—10^7$	10^{-6}	Discrete	$10^{-2}—10$
Electrical discharge	$1—10^4$	10^{-6}	»	10^{-3}

 0038-5670/82/110833-21$01.80

chemical compounds in the gaseous form.[219] In some cases, the small linewidth and good matching between the generator frequency and the absorption frequency of the material under investigation ensures selective dissociation of molecules containing a particular isotope of one of the elements, for example, the CO_2 laser ($\lambda \sim 10$ μm) has been used to separate sulfur isotopes in SF_6 (Ref. 220), osmium isotopes in OsO_4 (Ref. 221), and so on. On the other hand, collisionless multiphoton dissociation of molecules containing heavier elements (for example, uranium) involves the use of powerful pulsed generators producing radiation of longer wavelength ($\lambda \sim 16$ μm). The CF_4 ($\lambda \sim 16$ μm) and NH_3 ($\lambda \sim 12$ μm) gas lasers, pumped optically by the CO_2 laser, have been used to produce multiphoton dissociation of UF_6 (Refs. 222, 223), but selectivity with respect to the uranium isotopes was not achieved, probably because the CF_4 and NH_3 lasers could not be continuously tuned. New possibilities appear to have emerged as a result of SRS in parahydrogen pumped by the CO_2 laser.[224] Frequency tuning in the neighborhood of $\lambda \sim 16$ μm is possible in this case because the CO_2 laser frequency can be varied.

The separation of titanium isotopes in $TiCl_4$ by multiphoton dissociation requires the use of a powerful pulsed source of radiation operating near $\lambda \sim 20$ μm (Ref. 231).

The physical processes occurring in the far-infrared sources described below involve the use of lasers in one way or another. They make use of electrical-discharge or laser pumping of a gas placed in an optical cavity and capable of generating far-infrared radiation, or they rely on nonlinear optical processes.

One nonlinear-optics process resulting in the generation of far-infrared radiation is the separation of the wave with the difference frequency using the interaction between two monochromatic electromagnetic waves of different frequency sent to the specimen (crystal or gas cell) by an external source. Because the electrical properties of the specimen are nonlinear, this results in the appearance of an electromagnetic wave with frequency ω_3 equal to the frequency difference $\omega_1 - \omega_2$ between the waves incident on the specimen. The efficiency of this process becomes much higher when the condition $\mathbf{k}_3(\omega_3) = \mathbf{k}_1(\omega_1) - \mathbf{k}_2(\omega_2)$ is satisfied, and the amplitude of the wave with the difference frequency increases monotonically (in the stationary case) with distance from the crystal face in the interior of the specimen.

This process does not have a threshold in the incidentwave amplitude (independently of attenuation at the frequencies ω_1, ω_2, ω_3), and is a special case of parametric transformation of the frequency of electromagnetic radiation.[10] The wavevector relation $\mathbf{k}_1 = \mathbf{k}_2 + \mathbf{k}_3$ for interacting waves whose frequencies are related by $\omega_1 = \omega_2 + \omega_3$ is referred to as the phasematching condition.

An important special case of parametric frequency transformation in a nonlinear medium equipped with a cavity is that where the medium intercepts a strong electromagnetic wave (ω_1), and two others (ω_2, ω_3, where $\omega_1 = \omega_2 + \omega_3$) grow in the cavity. This is referred to as parametric generation[10] (process 1). Parametric amplification of the waves $\omega_2\omega_3$ in the nonlinear medium in which these waves are not attenuated does not have a threshold in the amplitude of the wave ω_1 incident on the nonlinear medium. When only one of the two waves ω_2, ω_3, for example, ω_2, is not attenuated, whereas the other is highly attenuated, the medium exhibits amplification without threshold for ω_2 (Ref. 9).

The other nonlinear optical process (process 2) occurs when a nonlinear medium (in a cavity or otherwise) intercepts one strong electromagnetic wave of frequency ω_1, whilst a wave of frequency ω_2 (Stokes satellite) grows in the nonlinear medium which is excited with characteristic frequency Ω. This is called stimulated Raman scattering (SRS). In this case, the frequencies are related by $\omega_1 = \omega_2 + \Omega$ (Ω is usually the frequency of vibration or rotation of molecules in the nonlinear medium). The corresponding phase matching condition $\mathbf{k}_1 = \mathbf{k}_2 + \Delta\mathbf{k}$ is then always satisfied in this process because the scattering medium takes up any momentum $\Delta\mathbf{p} = \hbar\Delta\mathbf{k}$. In principle, process 2 does not have a threshold in the amplitude of the incident wave (ω_1) if there are no losses at ω_2.

Stimulated scattering of light in noncentrally symmetric crystals by polaritons, i.e., collective excitations of the crystal lattice that are connected with the electromagnetic field and are active both in absorption and Raman scattering, can be described as SRS with allowance for polariton dispersion.[215]

In practice, processes 1 and 2 do have a threshold because the waves ω_2, ω_3 that grow in the parametric generator (or the wave ω_2 and the oscillations of the medium Ω in SRS) do exhibit attenuation (γ_2, γ_3). Each of these two processes will proceed if the amplitude E of the incident wave ω_1 is greater than the corresponding threshold E_{th}. In process 1, both ω_2 and ω_3, which appear as a result of parametric generation (with γ_2 and γ_3 of the same order), grow in the specimen, whereas the Stokes satellite ω_2 grows in the case of process 2.

The thresholds for processes 1 and 2 are similar:

$$E_{th}^{(1,2)} = \frac{1}{d}\frac{\sqrt{\gamma_2\gamma_3}}{\omega}.$$

where ω is of the order of the pump-wave frequency, $\gamma_{2,3}$ are the attenuation rates for waves ω_2 and ω_3 when process 1 is taking place, and $d = d_{(2)}$ (Ref. 9), where $d_{(2)}$ is the nonlinear polarizability of the medium ("quadratic" nonlinear susceptibility) in the expansion

$$\mathcal{P} = \frac{\varepsilon - 1}{4\pi}E + d_{(2)}EE + d_{(3)}EEE + \ldots$$

For process 2, γ_3 is the rate of attenuation of molecular vibrations and d is given by

$$d = \frac{\sqrt{\pi}N}{\omega}\sqrt{\frac{\omega_2}{\Omega}}\frac{\partial\alpha}{\partial Q},$$

where α is the polarizability and Q the optical phonon coordinate. For SRS in liquids and gases, d is defined by the "cubic" nonlinear susceptibility $d_{(3)}$ in the above expansion for the polarization in powers of E.

The threshold for an optically pumped laser (process 3) is determined by setting the attenuation γ of the generated wave equal to the growth rate in the inverted resonant medium

$$\gamma = \frac{\omega_2}{c} \operatorname{Im} \sqrt{\tilde{\varepsilon}},$$

where

$$\varepsilon = \frac{4\pi (n_2 - n_1) e^2}{i\nu\omega_2 M}.$$

If the energy of the pump wave is transformed into the energy of the upper laser level,

$$\frac{E^2}{4\pi} = \frac{n_2 \hbar\omega_1}{\tau},$$

the threshold is given by (we assume that $n_1 = 0$)

$$\frac{E_{\text{th}}^{(3)}}{\sqrt{8\pi}} \approx \sqrt{\frac{\hbar\omega_1}{4\pi e^2/M}} \sqrt{\gamma\nu}.$$

For gases we usually have $\sqrt{n\hbar\omega_1} \ll 1/d$ and the threshold for process 3 lies below that for process 2, and the optically pumped laser begins to operate earlier (for lower values of E) than for SRS. The only exception is provided by resonant SRS in which processes 2 and 3 can coexist (see Sec. 4).

Descriptions of the interaction between waves in a nonlinear medium are commonly based on the idea of plane waves with infinite wavefronts (in directions $\perp \mathbf{k}$). However, this is valid only when $a^2/\lambda L \gg 1$, where a is the transverse size of the interaction region and L is the wave interaction length.[48] When a nonlinear process results in the generation of a wave of relatively long wavelength ($\lambda \sim 1000$ μm) and highly focused pumping beams are utilized, it is essential to take into account diffraction divergence of the far-infrared radiation. On the other hand, for lasers operating in the far infrared (electrical-discharge or optically pumped), the use of waveguide techniques borrowed from the microwave region frequently results in an increase in the efficiency of such lasers.[86,186]

This review contains material referring only to generators of far-infrared radiation based on laser technology (nonlinear optical processes in solids and gases, electrical and optical pumping of gases) and does not cover generators using electron beams (backward-wave tubes, gyratrons, and so on).

2. SOURCES OF FAR-INFRARED RADIATION BASED ON THE ISOLATION OF THE DIFFERENCE FREQUENCY OF TWO LASERS

The isolation of the difference frequency of two lasers (generally two waves of different frequency) is possible only in a nonlinear medium without a center of inversion because it is only then that the medium has the "quadratic" nonlinear susceptibility $d_{(2)}$ that determines the mixing process. It is thus clear that the frequency subtraction process can be realized for two sources in noncentrally-symmetric crystals, many of which produce far-infrared radiation as a result.

We note that the addition (or subtraction) of the frequencies of three or more waves can also be performed in centrally-symmetric media, for example, in a gas, because these processes are due to nonlinear susceptibilities of the third order or higher. In particular, the authors of Ref. 226 have observed resonant four-photon mixing $\omega_1 + \omega_2 + \omega_3 = \omega_4$ in cesium vapor, and used the mixing process to produce optical radiation ($\lambda \sim 0.36$ μm). References to other papers of this type can be found in Ref. 232. The authors of Refs. 227 and 228 have suggested the use of a constant electric field as a way of breaking the central symmetry of gases and liquids, and the experimental mixing of two frequencies in hydrogen in an electric field was reported in Refs. 229 and 230. The wave produced as a result of the mixing process was found to lie in the near infrared ($\lambda \sim 2.4$ μm).

Theoretical analysis of the subtraction of the frequencies of two waves in a medium with quadratic nonlinear susceptibility $d_{(2)}$ is based on the so-called slow-amplitude equations,[10] which can be deduced from Maxwell's equations and the expansion of the polarization $\vec{\mathcal{P}}$ in powers of the electric field $\vec{\mathcal{E}}^0 = \mathbf{e}_n \mathcal{E}_n(t,x,y,z) \times \exp[i(\omega_n t - \mathbf{k}_n \mathbf{r})]$:

$$\mathcal{P}_i = \alpha_{ij}\mathcal{E}_j^0 + d_{ijk}\mathcal{E}_j^0\mathcal{E}_k^0 + \ldots; \qquad (2.1)$$

where $\vec{\mathcal{E}}^0$ is the electric field polarized along the vector $\mathbf{e}$, $\mathcal{E}$ is a slowly-varying amplitude, $\omega, \mathbf{k}$ are the frequency and wave vector, and the subscript n assumes the values 1, 2, 3, and refers to the radiation incident on the nonlinear medium ($n = 1, 2$) and the radiation with the difference frequency ($n = 3$), respectively. The linear (α_{ij}) and quadratic nonlinear (d_{ijk}) polarizabilities of the medium are tensors but, for a particular interaction in a chosen crystal, the nonlinear part of the polarization in (2.1), $d_{ijk}\mathcal{E}_j\mathcal{E}_k$, can be written in the form $d_{\text{eff}}\mathcal{E}(\omega_1)\mathcal{E}(\omega_2)$ after summation of terms with nonzero components of the tensor d_{ijk}.

The equations for the slow amplitudes lead to the following expression for the intensity at the difference frequency ω_3 (Ref. 10):

$$J_{\omega_3} = \frac{128\pi^3\omega_3^2}{c^3 n_1 n_2 n_3} d_{\text{eff}}^2 \times \frac{\exp(-2\gamma_3 x)\,|\exp[(-\gamma_1-\gamma_2-\gamma_3)x + i\Delta kx] - 1|^2}{(\Delta k)^2 + (-\gamma_1-\gamma_2+\gamma_3)^2} I_{\omega_1} I_{\omega_2}, \qquad (2.2)$$

where $I_{\omega 1,2,3} = nc\,|\mathcal{E}|^2/8\pi$ is the intensity of the radiation at the corresponding frequency, $n_{1,2,3}$ is the refractive index, $\gamma_{1,2,3}$ is the attenuation coefficient, and the difference $\Delta\mathbf{k} = \mathbf{k}_1 - \mathbf{k}_2 - \mathbf{k}_3$ is a measure of the departure from the phase-matching condition. When $2\gamma x \ll 1$, $\Delta k x \ll 1$, it is convenient to use, in practice, a simpler formula for the power emitted at the difference frequency, namely:

$$P_{\omega_3} = 128\pi^3 \frac{d_{\text{eff}}^2 \omega_3^2}{c^3 n_1 n_2 n_3} \frac{P_{\omega_1} P_{\omega_2}}{S} T_1 T_2 T_3 L_{\text{eff}}^2, \qquad (2.3)$$

where $P_\omega = IS$ is the power radiated at the particular frequency, S is the cross-sectional area of the interacting beams, $T = 4n/(n+1)^2$ is the transmission coefficient of the surface of the specimen, and L_{eff} is the effective interaction length obtained by integrating (2.2) along "filaments" parallel to $\mathbf{k}_3$ (see Fig. 1b).

In this chapter, we shall consider the generation of difference-frequency radiation in solids when this frequency lies in the far infrared. Equation (2.2) can be used to formulate the basic requirements that must be

satisfied by the crystal mixer in order to ensure high output power in the far infrared. They are: (1) the crystal must have second-order nonlinear susceptibility and its value of $d_{eff}^2/n_1n_2n_3$ must be high, (2) the crystal must be transparent to both the pump ($2\gamma_1 x, 2\gamma_2 x \ll 1$) and far-infrared radiation ($2\gamma_3 x \ll 1$), (3) the dispersion of the refractive index of the crystal must be sufficient to ensure phase-matching of the waves participating in the process ($\Delta k = 0$), and (4) the crystal must be highly stable under illumination, since the frequency-conversion occurs efficiently for high pump intensities.

The generation of far-infrared radiation by the frequency-difference laser method has been achieved in the following crystals: $LiNbO_3$ (Refs. 14, 15, 49), ZnO, ZnS, CdS, CdSe (Ref. 14), ZnTe (Ref. 12), ZnSe (Refs. 16, 34), GaAs (Refs. 22–32, 35), InSb (Refs. 17–20), $ZnGeP_2$ (Ref. 21), and CdTe (Ref. 36), and in the magnetoactive plasma of semiconductors.[37,212-214]

Published data on d_{eff} in the far infrared show a considerable spread. This is connected not only with the dispersion of d_{eff}, but also with the different experimental methods used to determine it. GaAs is a promising crystal for the generation of far-infrared radiation and has $d_{eff}^2/n_1n_2n_3 \sim 10^{-14}$ esu. This value is of the same order as for the most suitable crystal converters, but falls to 10^{-16} esu for other mixers.

In the crystal mixers used for frequency conversion, a lattice absorption band lies between the pump frequencies (ω_1, ω_2) and the difference frequency (ω_3). It follows that radiation losses are usually high in the shortwave part of the far infrared. Efficient generation of radiation with such frequencies can be achieved by cooling the crystal,[27,28] which leads to the narrowing of the lattice absorption band and to a reduction in the absorption of far-infrared radiation. Absorption in the far infrared may be different even for different samples of the same crystal (for example, for ZnSe $2\gamma_3$ (1000 μm) = 0.5 cm^{-1} and $2\gamma_3$ (200 μm) = 6 cm^{-1}; Ref. 16). However, for cooled crystals, for example, cooled GaAs, losses can be neglected throughout the range 100–1000 μm ($2\gamma_3 < 0.03$ cm^{-1}; Ref. 44).

Generation of far-infrared radiation by the frequency-difference method has been achieved in crystals even without the phase-matching condition being satisfied,[20,22,34,47] but the condition must be satisfied in order to increase the radiated power in the far infrared.

Let us now analyze ways of achieving the phase-matching conditions, i.e., $\omega_1 - \omega_2 = \omega_3$ and $\mathbf{k}_1 - \mathbf{k}_2 = \mathbf{k}_3$. Phase matching is often produced with the aid of birefringence.[11,13,21,52] This method exploits the fact that, by polarizing one of the waves (for example, ω_1) as the ordinary wave, and the other (ω_2), as the extraordinary wave, one can frequently satisfy the phase-matching condition for collinear wave propagation. However, this method is convenient only for birefringent crystals. Magnetoactive plasmas in semiconductors (Refs. 17, 18, 37, 53–55, and 212–214) are very favorable for satisfying the phase-matching conditions.

Phase matching was achieved in Ref. 23 by placing a nonlinear crystal in a waveguide. Another way of doing this is to vary the refractive indices by varying the temperature of the specimen.[19] Periodic variation of nonlinear susceptibility is put forward in Ref. 56 as a way of achieving phase matching.

Phase matching cannot be achieved in the case of normal dispersion in isotropic crystals. However, the lattice absorption bands (ω_0) and the anomalous dispersion bands of many crystals lie between the frequencies ω_1, ω_2 and the difference frequency ω_3: $\omega_1, \omega_2 > \omega_0 > \omega_3$. This can be exploited to achieve noncollinear phase matching in the frequency subtraction process in crystals with $n_3 > n_1, n_2$ (Refs. 16, 19, 24, 27), i.e., in crystals with anomalous dispersion. If we know the refractive indices, we can solve the wave vector triangle (see Fig. 1b) and find the angles θ and ϕ in the interior of the crystal for different combinations of ω_1, ω_2, and ω_3. Assuming that the angle θ is small and that $n_1 \simeq n_2$ and $(n_3 - n_1)/n_1 \ll 1$, we can readily show that[25]

$$\theta = \frac{\omega_3}{\sqrt{\omega_1\omega_2}}\sqrt{\frac{2\Delta n}{n}}, \quad \sin\varphi = \sqrt{\frac{2\Delta n}{n}} = \text{const}, \tag{2.4}$$

where $n \simeq n_1 \simeq n_2$ and $\Delta n = n_3 - n_1$.

The values of the angles for radiation from two CO_2 lasers mixed in a GaAs crystal are as follows: θ(deg) $= 2.5\times10^{-2}\omega_3(cm^{-1})$ and $\phi \simeq 22°$. The angle θ_{ext} between $\mathbf{k}_1$ and $\mathbf{k}_2$ outside the crystal is given by the obvious relation $\theta_{ext} = n\theta$.

High pump intensities tend to damage the crystal. Surface damage occurs first, and the threshold for this is determined by the properties of the particular material, the quality of surface polishing, and the conditions under which the crystal is used. It follows that the threshold for surface damage of the mixing crystal cannot be defined precisely. Moreover, damage may be begin not after the first but after one of the subsequent radiation pulses. Experience shows that, to achieve stable and prolonged operation of a far-infrared generator relying on the frequency difference between two lasers, the pump intensity in the semiconductor must be taken to be ~10^6 W/cm^2, and this can be increased by an order of magnitude by using dielectrics. In the narrow-gap crystal InSb, the intensity introduced into the crystal is restricted not by surface damage but by two-photon volume absorption of CO_2-laser radiation of about 10^5 W/cm^2 (Ref. 196).

Let us now estimate the far-infrared power generated by a system exploiting the frequency difference between two CO_2 lasers in GaAs. Substituting numerical values for the various quantities in (2.3) and taking $P_{\omega_1} \sim P_{\omega_2} \sim 10^6$ W, $S = 1$ cm^2, and $L_{eff} = 5$ cm, we obtain P_{ω_3}(W) $= 0.14\omega_3^2$ (cm^{-1}). For example, when $\omega_3 = 100$ cm^{-1} ($\lambda_3 = 100$ μm), we have $P_{\omega_3} = 1.4\times10^3$ W.

Lasers acting as pump sources in the frequency-difference method must produce powerful radiation at frequencies ω_1 and ω_2 such that $\omega_3 = \omega_1 - \omega_2$ lies in the far infrared. Since the far-infrared power is very dependent on the laser pump power, the pump sources are usually powerful pulsed lasers. The width of the spectrum produced by such sources in the far infrared is of the order of the width of the spectra of the laser pumps. For pulsed lasers, this is usually less than 0.1 cm^{-1}.

TABLE II. Parameters of far-infrared sources based on isolation of the difference frequency between two lasers.

Reference	P_{ω_1}, P_{ω_2}, Вт	P_{ω_3}, Вт	ω_3, $см^{-1}$	Tuning range $\Delta\omega_3$, cm^{-1}	Material	Pump laser	Plasma temperature
17	10^3	10^{-6}	100	—	InSb	CO_2	Cooling
19	$3\cdot10^2$	10^{-6}	100	—	InSb	CO_2	»
21	150	$1.7\cdot10^{-9}$	83	70—110	$ZnGeP_2$	CO_2	Room
	$1.8\cdot10^3$	$3\cdot10^{-8}$	30	—	GaAs	CO_2	»
37	80	$0.4\cdot10^{-8}$	100	—	Semiconductor plasma	CO_2	Cooling
212	$2\cdot10^3$, 10	$2\cdot10^{-6}$	101	—	Semiconductor plasma	Spin-flip laser	»
23	$4\cdot10^2$	$4\cdot10^{-6}$	1.79 1.81	—	GaAs	CO_2	»
24	$5\cdot10^4$	10^{-3}	100	—	GaAs	CO_2	»
27	25	$2\cdot10^{-7}$	100	10—140	GaAs	CO_2	»
28	$2\cdot10^5$	$2\cdot10^{-2}$	100	5—140	GaAs	CO_2	»
31	$2\cdot10^5$	0.6	100	—	GaAs	CO_2	»
32	$1.3\cdot10^5$	50	100	5—140	GaAs	CO_2	»
32	$2\cdot10^5$	$4\cdot10^{-2}$	100	5—140	GaAs	CO_2	»
16	$2\cdot10^5$	0.1	25	2—50	ZnSe	CO_2	Room
29	10^5	10^{-2}	30	2—100	GaAs	CO_2	»
30							
45	$3\cdot10^5$	10	25	2—30	GaAs	CO_2	»
49	$3.5\cdot10^5$	10^{-3}	—	10.9—18.6	$LiNbO_3$	Ruby	»
14	$6\cdot10^5$	10^{-2}	20	20—127	$LiNbO_3$	Dye	»
		$2\cdot10^{-2}$	20	20—95	$LiNbO_3$	»	Different phase-matching contitions
		0.8	50	40—160	$LiNbO_3$	»	
14	$6\cdot10^5$	$1.4\cdot10^{-2}$	190	—	ZnO	»	Room temperature
14	$6\cdot10^5$	$3\cdot10^{-3}$	180	—	CdS	»	»
14	$6\cdot10^5$	$0.74\cdot10^{-3}$	91	—	ZnS	»	»
14	$6\cdot10^5$	$0.15\cdot10^{-3}$	150	—	CdSe	»	»

A far-infrared source with linewidth of 100 kHz and fine tuning capability in excess of 50 MHz was developed in Ref. 27 using the CO_2 lasers. Experiments with the generation of far-infrared radiation have also used the following pump sources: ruby laser,[11,12] neodymium glass laser,[13] dye lasers,[14,15] CO_2 lasers,[16-32], and the spin-flip laser.[33,212-214]

Table II lists the parameters of far-infrared sources based on isolating the difference frequency between two lasers.

Sources of radiation based on the mixing of the frequencies of electromagnetic waves in nonlinear crystals usually consist of the following elements (Fig. 1). The radiation from the two lasers 2 is first tuned to the frequencies ω_1 and ω_2 by dispersive elements 1 (for example, diffraction gratings) and then conveyed to the mixing crystal 4 by mirrors 3. Radiation of frequency $\omega_3 = \omega_1 - \omega_2$ is recorded by the detector 5. [We note that there is an extensive literature on the detection of far-infrared radiation (see, for example, Refs. 197–206) from which researchers can choose the particular detector for their own experiments.] Particular systems for the generation of far-infrared radiation may depart from this precise scheme. For example, in collinear phase matching, one of the lasers can conveniently be used to produce radiation of two frequencies, ω_1 and ω_2, propagating in the same direction.[14,38] An original method of generating far-infrared radiation is described in Refs. 50 and 51, where rectification of picosecond laser pulses is employed.

Let us now consider in detail sources of far-infrared radiation that exploit the mixing of radiation from two CO_2 lasers. As compared with other methods, this has the advantage of the simplicity of the CO_2 laser and the fact that it is capable of generating high-power far-infrared radiation.[16-32,35-37]

The CO_2 laser is of considerable interest as a source of pumping radiation for the generation of far-infrared radiation. This is so because the CO_2 laser radiation originates from a set of vibrational-rotational transitions in the CO_2 molecule that lie in the range 920–1060 cm^{-1}, and the separation between the rotational sublevels is of the order of a few reciprocal centimeters.[39] The difference frequency that can be obtained with two CO_2 lasers is thus seen to lie in the range 2–140 cm^{-1} (5000–70 μm). By combining different frequencies of two CO_2 lasers, it is possible to produce more than 3000 discrete frequencies in this range. Use of the high-pressure CO_2 laser in which collisional broadening gives rise to the overlap between rotational sublevels[40] offers the possibility of a continuously tunable source for the far infrared. The development of compact cw CO_2 lasers has led to the possibility of continuous generation in the far-infrared region.[27]

In Refs. 212–214, the pump radiation from the CO_2 laser of frequency ω_1 is directed onto a crystal in which it undergoes stimulated Raman scattering by conduction electrons in a semiconductor located in a magnetic field (spin-flip laser). The Stokes component of frequency ω_2 is then mixed with the radiation of the reference laser of frequency ω_1, and far-infrared radiation of frequency $\omega_3 = \omega_1 - \omega_2$ is produced. This method is interesting because it is capable of continuous frequency tuning in the far-infrared.

The following single crystals have been used as nonlinear media in sources of far-infrared radiation using the CO_2-laser frequency conversion: InSb (Refs. 17–20), $ZnGeP_2$ (Ref. 21), GaAs (Refs. 22–32, 35), ZnSe (Ref. 16), and CdTe (Ref. 36). The magnetoactive plasma in InSb (Ref. 37) has also been used. The GaAs crystal occupies a special position among these materials. It satisfies the requirements imposed on mixing crystals, and is transparent to both far infrared and to 10-μm radiation. The refractive index and the absorption coefficient of GaAs at different temperatures are well known.[41-43] The dispersion of GaAs is such that it can be used to produce noncollinear phase-matching between interacting waves[28] (Fig. 1). GaAs exhibits the relatively high degree of nonlinearity that is important for the separation of the difference frequency.[23] With suitable surface treatment, the GaAs crystal has a high threshold for surface damage.[44] Good-quality GaAs

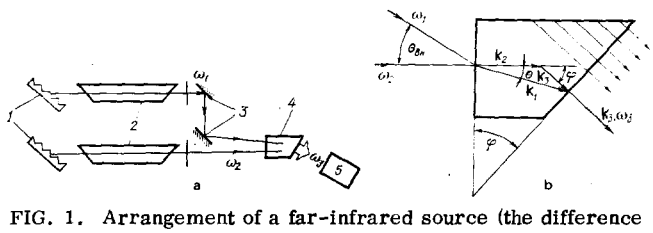

FIG. 1. Arrangement of a far-infrared source (the difference frequency between two lasers is isolated) (a) and noncolinear phase matching (b).

crystals are widely used and are manufactured by Soviet industry.

Figure 1 shows an experimental arrangement for the generation of far-infrared radiation that exploits the isolation of the difference frequency between two CO_2 lasers in a GaAs crystal. Since noncollinear phase matching is produced in the GaAs crystal, the exit face of the crystal is cut at an angle of 21° in order to prevent total internal reflection of the far-infrared radiation at this face.

It is important to note that sources of far-infrared radiation that are based on the isolation of the difference frequency between two CO_2 lasers in the GaAs crystal have relatively small dimensions and can be placed on a laboratory table. Thus, the two CO_2 lasers used in Ref. 32, which generated 2 MW (this figure is readily achieved with compact CO_2 TEA lasers), produced far-infrared radiation that could be tuned within the range 5–140 cm^{-1}, and the output at 100 μm (100 cm^{-1}) was about 4 kW. However, the GaAs used in this work was kept at cryogenic temperatures, which made the experiment technically more complicated. Effective generation in the region 30-2 cm^{-1} (300–5000 μm) can be achieved by using a GaAs crystal at room temperature,[29,30] which makes such sources of far-infrared radiation relatively simple to fabricate and use. Systems of this kind will readily produce 10 W at 400 μm (25 cm^{-1}) when pumped with 0 3 MW of radiation. The width of the far-infrared spectrum produced by this type of source can be varied by varying the spectrum of the radiation generated by the CO_2 pump lasers. Thus, for example, the "hybrid" CO_2 laser[46] can be used as the pump to produce a linewidth of about 50 MHz in the case of pulsed generation.

3. POLARITON GENERATORS OF FAR-INFRARED RADIATION

As noted in the Introduction, SRS processes in gases, which are governed by the third-order nonlinear susceptibility $d_{(3)}$, so that the pump frequency does not enter into resonance with any of the allowed transitions in the scattering medium, have been used to generate radiation with wavelength up to 20 μm. Stokes radiation near 17 μm can be produced by using this process in parahydrogen pumped by a pulsed CO_2 laser. This process is accompanied by a rotational transition in parahydrogen with $\Delta\nu \sim 354$ cm^{-1} (Ref. 224). In another case,[226] SRS was observed in cesium vapor for the second harmonic (3470 Å) of a mode-locked ruby laser. The corresponding Stokes wavelength was about 20 μm and the process was accompanied by an electron transition in cesium.

The wavelength of the Stokes radiation cannot be increased further by suitably choosing the frequency of the laser and of the transition in the scattering medium because of the quadratic reduction in the SRS gain with decreasing frequency of the Stokes radiation[9] and, consequently, the increase in the SRS threshold (in the sense noted in the Introduction).

The fact that SRS processes could be used to generate far-infrared radiation became clear as a result of the experimental realization of resonant SRS in gases (Sec. 4). The threshold for resonant SRS (RSRS) is sufficiently low for practical purposes, which is a consequence of the resonance between the pump radiation and one of the allowed transitions in the scattering medium.[137-139,207,209-211]

Parametric light generators (PLG) are based on parametric superluminescence,[215] which is determined by the quadratic nonlinear susceptibility $d_{(2)}$, and can be used to generate radiation with wavelength up to 16 μm.[58,59] The frequencies of the pump wave (ω_1) and the PLG radiation (ω_2, ω_3) are then found to lie well away from the lattice absorption frequencies of the crystal. Existing crystals can be used to extend this range to 22 μm.[74] Parametric generators are pumped by lasers operating in the visible or near-infrared ranges, in which case a cavity is used to produce negative feedback through the waves with frequencies ω_2 and ω_3. The PLG will operate when the following phase-matching conditions are satisfied

$$\omega_1 = \omega_2 + \omega_3, \quad \mathbf{k}_1 = \mathbf{k}_2 + \mathbf{k}_3, \tag{3.1}$$

and the collinear arrangement ($\mathbf{k}_1 \| \mathbf{k}_2 \| \mathbf{k}_3$) is common. The frequencies ω_2, ω_3 are varied by varying the phase-matching conditions and suitably choosing $n_1(\omega_1)$, $n_2(\omega_2)$, $n_3(\omega_3)$ for the dispersion characteristics of the nonlinear PLG element. The parametric generation threshold (in the sense indicated in the Introduction) is determined by the condition demanding that the gain must be equal to the losses.[9,10,57,58] A reduction in one of the frequencies generated by the PLG (for example, ω_3 brings the frequency ω_3 close to the lattice absorption band of the nonlinear crystal; the wave of frequency ω_3 becomes strongly coupled to the crystal lattice vibrations and is referred to as a polariton (polariton mode).[70] The wave of frequency ω_3 is then strongly absorbed and this leads to a higher parametric generation threshold. The phase-matching conditions cannot be satisfied in collinear geometry in this frequency range.

If, however, the wave ω_3 is separated on the dispersion curve $n(\omega)$ from the waves ω_1, ω_2 by the lattice absorption bands, the noncollinear phase-matching condition can be satisfied (the vectors $\mathbf{k}_1, \mathbf{k}_2, \mathbf{k}_3$ form a triangle).[60-69] The approach of the frequency ω_3 to the lattice absorption band of a nonlinear crystal gives rise to a specific nonlinear interaction between waves in this frequency band, which is referred to as stimulated scattering by the polariton.[215] The vibrations of the crystal lattice in the polariton mode of crystals without a center of inversion (but with the quadratic nonlinear susceptibility $d_{(2)}$!) are Raman-active,[45] so that SRS determined by the nonlinear susceptibility $d_{(3)}$ is possible in this polariton mode. It is thus clear that nonlinear interaction between waves during stimulated scattering by the polariton is determined by a combination of $d_{(2)}$ and $d_{(3)}$, and can be described as SRS determined by the nonlinear susceptibility d_3^{eff} (Ref. 215). However, $d_{(3)}$ has a resonance at the frequency of the optical phonon in the crystal, and provides an appreciable contribution to polariton scattering only in a narrow frequency band near this resonance. In the frequency region well away

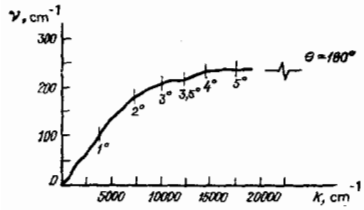

FIG. 2. Polariton dispersion in lithium niobate: $\nu = 1/\lambda_3$, $k = 2\pi n_3/\lambda_3$, numbers shown against graphs are the values of the angle θ corresponding to phase matching for the ruby laser frequency.

from resonance, where the nonlinear phase-matching condition is satisfied, stimulated scattering by the polariton can be described as parametric generation.[215]

Experimental devices in which stimulated scattering by polaritons is exploited are referred to as polariton generators, and the wave ω_2 is called the Stokes wave[62] (ω_1 is the pump frequency).

The $LiNbO_3$ crystal is at present the most suitable nonlinear crystal for polariton generators of far-infrared radiation. The absorption coefficient of $LiNbO_3$ in the visible range is $2\gamma_{1,2} \approx 0.08$ cm^{-1}, and the corresponding refractive index is $n_{1,2} = 2.2$ (Ref. 71). The dispersion of the 248-cm^{-1} polariton is shown in Fig. 2 (Ref. 72). It is clear from these data that, when the pump wave propagates at right-angles to the optic axis of $LiNbO_3$ with the electric vector $\vec{\mathscr{E}}_1$ parallel to the optic axis, the condition given by (3.1) can be satisfied for the three extraordinary waves, i.e., noncollinear phase-matching is achieved (Fig. 3b). The expressions for the matching angles can be obtained by analogy with phase matching for two waves mixed in an isotropic medium:

$$\theta = \frac{\omega_3}{\omega_1}\sqrt{\left(\frac{n_3}{n_1}\right)^2 - 1}, \quad \sin\varphi = \sqrt{1 - \left(\frac{n_1}{n_3}\right)^2}. \tag{3.2}$$

It is important to note that, when $\Delta n/n$ is small, the expression given by (3.2) becomes identical with (2.4). Substituting numerical values into (3.2), we find that the angles θ and ϕ for $LiNbO_3$ in the interior of the crystal in a polariton generator pumped by a ruby laser are as follows: $\theta(\text{deg}) = 0.01\omega_3$ (cm^{-1}) and $\phi \simeq 60°$. Since the angle ϕ is greater than the angle of total internal reflection, the crystal is cut at the angle ϕ to allow the far-infrared radiation to escape.

Figure 3a shows a typical experimental arrangement for the generation of far-infrared radiation by stimulated scattering by a polariton. The lens L focuses the

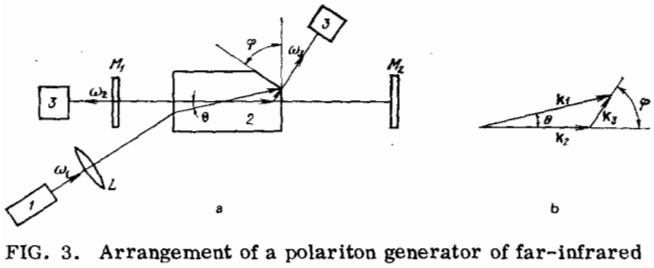

FIG. 3. Arrangement of a polariton generator of far-infrared radiation (M_1, M_2—mirrors, L—lens; 1—laser pump, 2—nonlinear crystal, 3—diagnostic equipment) (a), and phase matching (b).

giant-pulse laser on the crystal. Mirrors M_1 and M_2 form a resonator for the Stokes radiation ($\omega_2, \mathbf{k}_2$) (in some experiments, plane-parallel crystal faces are used as the mirrors). The Stokes radiation and the far-infrared radiation ($\omega_3, \mathbf{k}_3$) are intercepted by a diagnostic set, and the far-infrared radiation is wavelength-tuned by varying the angle θ between the axis of the cavity formed by the mirrors, M_1, M_2, and the direction of propagation of the pump wave.

Polariton generators producing far-infrared radiation are being investigated by studying the direct emission of far-infrared waves and of emission at the Stokes frequency. Tunable Stokes radiation was first observed in Ref. 65. In that work, a ruby laser pulse ($\lambda_1 = 0.6943$ m), 2×10^{-8} s long, was focused in an $LiNbO_3$ crystal located in a Stokes resonator, at a power density of up to 100 MW/cm^2. The Stokes frequency ω_2 was varied by varying the angle θ. The emission at frequency ω_2, which corresponded to scattering by the 248-cm^{-1} polariton, could be retuned by 36 cm^{-1} by varying the angle θ.

The frequency ω_2 and, consequently, the frequency ω_3 calculated from (3.2), do not always correspond to the angle θ between the resonator axis and the direction of propagation of the pump wave $\mathbf{k}_1$. The reason for this is that, because of the high gain, the Stokes emission ($\omega_2, \mathbf{k}_2$) may not be collinear with the resonator axis. It builds up from the noise level after a few passes in the nonaxial direction, with the frequency given for this direction by (3.2). This direction is determined by the ratio of the gain at frequency ω_2 to losses in the resonator. These properties of the polariton generator are investigated in detail in Ref. 68.

Generation of far-infrared radiation by scattering ruby-laser radiation by the 248-cm^{-1} polariton in $LiNbO_3$ crystals was investigated in Refs. 63, 64, 67, and 69. The radiation was tuned in the range 238–50 μm (42–200 cm^{-1}) at a power of a few watts, for which the pump power was a few megawatts. The expansion of the tuning range toward shorter wavelengths is restricted by the polariton frequency. At the other end of the spectrum, it is restricted by difficulties in introducing the pump radiation into the Stokes resonator. The linewidth of the far-infrared radiation was determined from the width of the Stokes line and was found to be a few tenths of cm^{-1}. This is in good agreement with the Manley-Rowe relation between the power carried by the Stokes radiation (P_2) and the power difference $P_2 = (\omega_2/\omega_1)(P_{1\text{in}} - P_{1\text{out}})$ between radiation entering and leaving the crystal, respectively. Since the far-infrared radiation is strongly absorbed in the crystal, the relationship between the Stokes and the far-infrared radiation must include a term representing this absorption:[9,61,65]

$$P_3 = P_2 \frac{\omega_3}{\omega_2} \frac{1}{1 + (2\gamma_3/g_S \cos\varphi)},$$

where g_S is the Stokes gain. This formula is in good agreement with experimental data.

The interval in which the far-infrared radiation can be tuned can be extended toward longer wavelengths by replacing the ruby laser with a laser capable of gen-

erating radiation of longer wavelength. According to (3.2), the angle θ increases with increasing wavelength, so that it is eventually possible to introduce the pump radiation into the external Stokes resonator at angles ensuring that the matching condition for the generation of long-wavelength radiation is satisfied. The pump source used in Ref. 65 was a neodymium-glass laser ($\lambda_1 = 1.06$ μm), whose radiation was focused in an $LiNbO_3$ crystal at power levels of up to 50 MW/cm^2. Far-infrared radiation was thus produced in the range 153–708 μm (14.1–65.4 cm^{-1}) and was recorded at power levels of 10–100 W, depending on wavelength.

Because the threshold for stimulated scattering by polaritons is high ($I_{th} \sim 4\times10^7$ W/cm^2), the pump source is commonly a powerful Q-switched laser producing short pulses (10–20 nsec). This ensures that the Stokes emission used to achieve the feedback loop only just succeeds in building up from the noise level to the recorded value during the presence of the pulse. The nonstationary behavior of polariton generators was investigated in Ref. 69.

It is important to note that far-infrared radiation has also been generated in quartz pumped by a ruby laser.[66] The quartz crystal was cooled to 10 °K, but no indication is given in Ref. 66 of the power recorded in the far-infrared range. Analysis of the experimental data indicates that the wavelength of the radiation was $\lambda_3 \sim 75$ μm (130 cm^{-1}).

The spin-flip Raman laser is, in a certain sense, close to the FIR polariton generator.

This laser is based on SRS that involves a transition of magnetized conduction electrons between spin sublevels of Landau levels of a semiconductor cooled down to about 20 °K (frequently InSb).[233] The frequency ω_{sp} of the scattering transition is given by $\omega_{sp} = \omega_L - \omega_S = (2/\hbar) g \mu_B H$, where H is the magnetic field, ω_L is the pump frequency, ω_S is the Stokes frequency, μ_B is the Bohr magneton, and g is the Landé factor. The spin-flip Raman laser is usually pumped either by a CO_2 laser ($\lambda_1 \sim 10$ μm) or a CO laser ($\lambda_2 \sim 5$ μm). The wavelength λ_S of the Stokes radiation can be varied continuously by varying the magnetic field. The spin-flip laser can therefore be tuned near $\lambda_1 \sim 10$ μm ($\lambda_S > \lambda_1$) in the case of the CO_2 laser pump and near $\lambda_2 \sim 5$ m ($\lambda_S > \lambda_2$) in the case of the CO laser pump.

The electron transition between spin sublevels in the case of SRS with spin flip is a collective excitation in the semiconductor, connected with the electromagnetic wave.[73] The extraction of the "spin" wave with frequency ω_{sp} lying in the far infrared, which could be varied by varying the magnetic field, was achieved experimentally in Ref. 73. This enables us to place the spin-flip laser in the same context as the FIR polariton generator.

Along with the advantages of the FIR polariton generator (such as the use of a single pump laser, which need not be frequency tuned, and the continuous frequency tuning of the far-infrared radiation), there are also difficulties in its experimental realization. The difficulties are connected with the fact that the experimental conditions must be chosen so that the pump laser power is higher than the threshold for stimulated scattering by the polariton and, at the same time, lower than the threshold for damage to the crystal. The FIR polariton generator cannot be produced if the damage threshold lies below the threshold for stimulated scattering by the polariton.

4. OPTICALLY-PUMPED GAS LASERS FOR THE FAR INFRARED

A. General principles of operation of optically pumped gas lasers

Optically pumped lasers operate in different regions of the spectrum, including the far infrared (between $\lambda = 30$ μm and $\lambda = 2000$ μm). The working medium can be a solid, a liquid, or a gas.

(1) *Optically-pumped three- and four-level lasers.* These lasers can be pumped by broad-spectrum lamps or by lasers. Lasers designed for the far infrared incorporate a gaseous active medium pumped by a laser.[75,78] Absorption of the pump radiation by the working gas produces a population inversion Δn_{ij} between the upper working level i and the lower level j, so that a gain γ is produced at the transition frequency ν_{ij}. Figure 4 shows different variants[78] of the three- and four-level optically-pumped laser. In the three-level scheme, inversion is achieved as a result of the "population" of the upper laser state i or as a result of the depletion of the lower state j (Fig. 4a, b). Population inversion can be achieved in the four-level scheme by successively taking the active particles first to level l and then from level l to level i (Fig. 4c). This is two-level pumping (ν_{kl} and ν_{li}). The laser will operate in this way even when the intermediate level l is shifted from the resonance position to the position l', or when the level l is absent altogether. The pumping efficiency in the latter cases depends on the nonlinear properties of the medium. In the four-level scheme shown in Fig. 4d, the medium is excited (level i is populated) as a result of a radiative or radiationless transition $l \to i$ in the presence of a pump of frequency ν_{kl}.

The operation of the above lasers may be accompanied by SRS processes if the working medium has sufficiently nonlinear properties.

(2) *Characteristic power.* Intensive generation (~1 MW) can be achieved in the far infrared by exciting the working gas with short (compared with the relaxation time) powerful laser pulses. In the case of stationary (or quasistationary) pump power, the resulting stationary far-infrared radiation can range from a few microwatts to a few milliwatts.[78]

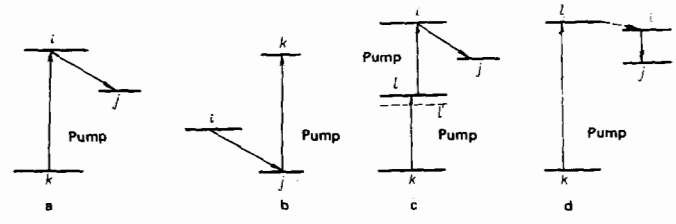

FIG. 4. Principle of different optically-pumped lasers.

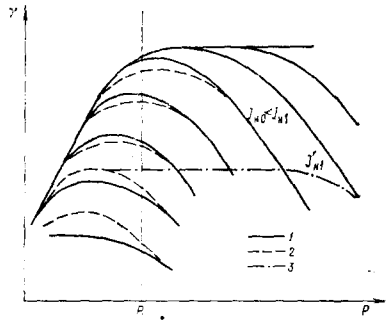

FIG. 5. Laser gain as a function of pressure for different pump intensities: 1—broad-spectrum pump; 2—single-frequency pump, 3—pump frequency detuned from the frequency of the transition in the working gas.

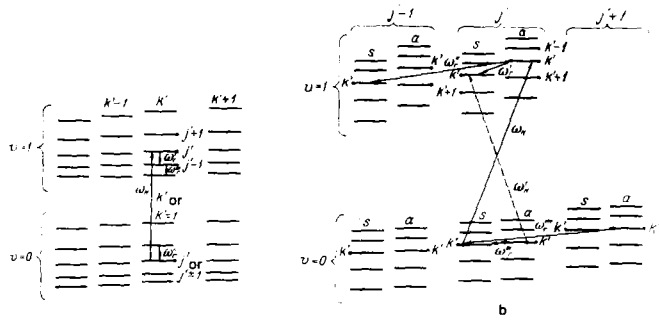

FIG. 6. Partial level scheme of CH_3F (a) and NH_3 (b).

(3) *Gain and its dependence on pressure and pump power.* The gain (in cm^{-1}) of the active medium is given by[77]

$$\gamma(\nu) = F_{ij}\left(n_i - n_j\frac{g_i}{g_j}\right)S(\nu, \nu_{ij}). \qquad (4.1)$$

where n_i and n_j are the populations of levels i and j (in cm^{-3}; see Fig. 4), g_i and g_j are the statical weights of states i and j, and S is the line profile (in Hz^{-1}). The quantities F_{ij} can be expressed in terms of the dimensionless oscillator strength f_{ij} or in terms of the transition wavelength λ_{ij} and one of the Einstein coefficients A_{ij} (or B_{ij}), or in terms of the wavelength λ_{ij} and the transition dipole moment μ_{ij}:

$$F_{ij} = 2{,}654\cdot10^{-2}f_{ij} = 3{,}979\cdot10^{-10}\lambda_{ij}^2A_{ij} = \frac{hB_{ij}}{\lambda_{ij}} = 1{,}2478\cdot10^{-4}\frac{\mu_{ij}^2}{\lambda_{ij}}, \qquad (4.2)$$

where A_{ij} is in s^{-1}, μ_{ij} is in debyes, λ_{ij} is in μm, and h is the Planck constant. The gain of the optically pumped active medium (gas) depends on its pressure, the pump intensity, and the difference between the frequency of the pump radiation and the center of the gas absorption line. Figure 5 shows a diagram illustrating the dependence of γ on and the pressure intensity of the pump. It also shows the effect of the width of the pump spectrum and of the detuning of the pump radiation from the center of the absorption line.[78] In Fig. 5, p_1 is the pressure at which collisional broadening of the line (ν_{ij} transition) is comparable with the Doppler broadening. The pressure p_1 is usually of the order of a few torr at room temperature. For a strong enough pump (in the limit, for a pump saturating the $k \to i$ transition) and for $p < p_1$, the gain γ increases with increasing p because of the increase in the density of the active particles. For increasing $p > p_1$, and when the pump intensity is high enough to saturate the transition, the number of active particles is compensated by the increase in the collisional linewidth. If saturation has not been reached ($I \leq I_s$), the gain γ will be reduced by collisional broadening of the modified line (of course, for times $\tau \ll \tau_{ij}$). Broken curves show the change in the corresponding relationships for a "single-frequency" pump, i.e., a pump with a narrow spectrum. At low pump intensities, the narrower pump spectrum reduces the spread over the active-particle velocities and, consequently, leads to a narrowing of the amplified line and to an increase in γ. For high intensities, the single-frequency pump "depletes" the initial state, and a valley appears on the Doppler profile of level k. However, there is then a greater velocity spread in the state i because of the dynamic Stark effect[90] which broadens the level i, so that γ has a lower value as compared with the case of a broad-spectrum pump. The effect of frequency detuning of the pump from the absorption-line center is demonstrated by the dot-dash curve (I'_{s_1}), which corresponds to the solid curve (J_{s_1}) in the absence of detuning. It is clear from Fig. 5 that the optimum conditions for reaching γ_{max} for minimum pump intensity are $p \sim p_1$, $I \sim I_{s_0}$ (without detuning, the pump spectrum is relatively broad).[78]

(4) *Levels and selection rules.* Molecular-gas lasers operate in the far infrared (λ = 30–2000 μm), where the working transition $i \to j$ is purely rotational (for diatomic molecules or for molecules in the form of an asymmetric or a symmetric top, other than NH_3), or inverted, or inverted-rotational (for NH_3; Ref. 78). Figure 6a shows an example of a vibrational-rotational level scheme for a molecule in the form of a symmetric top (for example, CH_3F), together with the pump and generation transitions in the far infrared.[75] The symbols v' and $v'+1$ label vibrational states of a given vibrational mode of the molecule (in the lower electron state), and the "sublevels" corresponding to subscripts j and k represent the rotational structure (k labels the component of the angular momentum along the axis of the molecule). For linear molecules, $k = 0$, and the scheme shown in Fig. 6a is valid for them in all other respects. Figure 6b shows the level near the vibrational ground state ($v = 0, 1$) of the ν_2 mode of ammonia, NH_3. The NH_3 molecule is a symmetric top, each vibrational level of which is split into two levels corresponding to the symmetric and asymmetric states (inversion splitting). The size of the inversion splitting for the mode ν_2 increases with increasing v, and the level energy decreases with increasing k.[81-84] Inversion splitting of vibrational levels, which distinguishes the NH_3 molecules from other symmetric-top molecules, is a consequence of the "tunneling" of the N atom through the plane of the triangle formed by the hydrogen atoms in NH_3.

The vibrational state of molecules having the form of the asymmetric top (for example, H_2O, CH_3OH, and so on) can also have a vibrational (j, k) structure, and degeneracy is absent for levels with indices $-k$, $+k$ (in contrast to symmetric tops). The selection rules (for symmetric tops) governing vibrational-rotational tran-

sitions in absorption (pump ω_p) are illustrated in Figs. 6a ($\Delta v = 1$, $\Delta j = 0, \pm 1$, $\Delta k = 0, \pm 1$). Selection rules for vibrational-rotational transitions in NH_3 in absorption (pump $\omega_p \sim \omega_p'$) are illustrated in Fig. 6b ($\Delta v = 1$, $\Delta j = 0$, ± 1, $\Delta k = 0$, $s \nrightarrow a$ or $a \nrightarrow s$). For linear molecules, $k = 0$, so that pump absorption corresponds to $\Delta v = 1$, $\Delta j = 0$, ± 1.

When the radiation is emitted as a result of purely vibrational transitions, the selection rules for linear molecules become $\Delta j = -1$, whereas, for symmetric-top molecules, $\Delta j = -1$, $\Delta k = 0$. Even cascade generation is possible (for example, in NH_3, etc.), in which the radiating transition produces an inverted population on the lower laser level, as illustrated in Fig. 6a (ω_L' and ω_L''). For NH_3 (see Fig. 6b), the selection rules in emission are $\Delta j = 0, \pm 1$, $\Delta k = 0$, $s \nrightarrow a$ or $a \nrightarrow s$; here, $\Delta j = 0, 1$ are possible because of inversion splitting of the levels. For asymmetric-top molecules, the selection rules become less stringent as compared with symmetric molecules, so that the number of absorption lines associated with vibrational-rotational transitions in asymmetric molecules becomes much greater.[78]

(5) *Optimal pressure.* Optically pumped FIR lasers usually operate at frequencies between 0.01 and a few torr (near the optimum for γ). The working pressure cannot be increased (to achieve higher power) for two reasons: firstly, because of collisional relaxation of the upper state or, equivalently, because of the rapid establishment of the equilibrium population distribution over rotational levels (with temperature of the order of the translational temperature T_t of the gas); secondly, there is the self-absorption of the generated radiation by the rotational structure of the vibrational ground state, which has a Boltzmann population distribution. A reduction in pressure reveals a small relative shift in the vibrational structures of the vibrational ground state as compared with the higher-lying states, so that self-absorption decreases as a result of departure from resonance. The pump and generation scheme shown in Fig. 4b, in which each rotational transition is a k-multiplet (for example, for symmetric-top molecules) is particularly sensitive to self-absorption.[78]

(6) *Polarization.* An interesting feature of optically pumped FIR lasers is the fact that, when the pump is linearly polarized, the generated radiation is usually also linearly polarized (see, for example, Ref. 78). The degree of polarization of the laser emission in the case of a linearly polarized pump is high when the pump excites levels with $j \gg k$; in the opposite case ($j \sim k$), the degree of polarization of the laser radiation is low. This type of dependence of the polarization of laser radiation on j and k is connected with the reduction in the time of collisional reorientation of excited molecules with $j \sim k$, as compared with molecules for which $j \gg k$. The relationship between the polarizations of the pump and of the laser radiation (i.e., the angle between them) depends on whether the selection rules for j are the same for generation and for the pump.[78] When $|\Delta j|$ for the pump is equal to $|\Delta j|$ for generation, the two polarizations are parallel. When the two moduli are not equal, the polarizations are orthogonal.

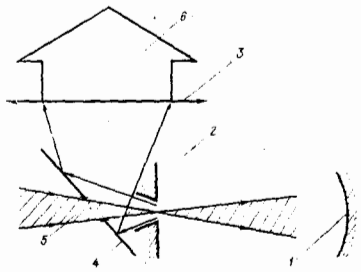

FIG. 7. Optics of a far-infrared laser: 1—spherical mirror, 2—plane mirror with appertures, 3—lens window, 4—beam separator, 5—pump radiation, 6—far-infrared radiation.

B. Experimental techniques

A great variety of experimental arrangements has been used to observe generation by optically pumped gases.

(1) *Optical scheme.* Figure 7 shows a typical arrangement for the generation of far-infrared radiation by an optically pumped gas. The system is usually placed in an evacuated chamber, 1 m long (along the resonator axis). The resonator mirrors are usually inserted into the chamber in order to avoid the absorption of the generated radiation by the atmosphere in the resonator. The resonator filled with the optically pumped gas is coupled to the pump radiation through an aperture in one of the mirrors, on which the pump beam is focused. The generated radiation, directed by a horn, leaves through the same aperture. The pump and the generated beams are separated by inserting a beam separator with a central aperture. The pump beam has a small transverse cross section and passes through the beam-separated aperture, whereas the generated radiation which forms a large spot on the beam separator is reflected and leaves the generator through a lens.

Since the far-infrared radiation leaves through the same aperture in the mirror as the pump, it is necessary to employ a conical horn in order to reduce the divergence of the generated radiation, in the same way as is done in microwave technology. The use of a single coupling aperture for the pump and the infrared radiations complicates the optimization of the coupling process. The optimization procedure is easier to apply when the resonator is coupled to the generated radiation by a mirror which completely reflects the pump radiation but is partially transparent to the far infrared (hybrid mirror[85]). Coupling between the resonator and the pump radiation is achieved, as before, through a small aperture in a metal mirror.

When the gas is pumped by a powerful CO_2 TEA laser, so that the frequency of the absorbing transition in the gas is sufficiently close to the pump frequency, it is possible to reach the so-called superradiant state.[100,120-122] The pump radiation is then absorbed in a single pass through the 1–5 m cell (diameter up to 10 cm), and the far-infrared radiation is generated without the use of the mirrors. The generated radiation is separated in this scheme by a filter at the end of the cell, which is opaque to the pump radiation.

(2) *Waveguide lasers.* With optically-pumped cw

lasers, we encounter the well-known difficulty that the rate of population of the lower laser level is inadequate. Since deactivation of particles occupying the lower laser level occurs on the walls (as a result of diffusion), the diameter of the tube containing the active medium must be small. This has led to the development of the "waveguide" resonator for the far-infrared radiation, which is still an *open* resonator for the pump radiation. A typical arrangement is that employing a waveguide in the form of a metal tube with an internal diameter of about 12 mm. This laser will operate at higher working gas pressures.[86] A tube diameter of 25 mm is required for lasers working at $\lambda \sim 1$ mm or higher. Another way of increasing the rate of depopulation of the lower laser level is to use a suitable buffer gas in the required concentration. For example, in the CH_3F laser, the introduction of C_6H_{14} in the ratio of 1 : 1 gives rise to an increase in the generated power by a factor of 1.5. Buffer gases in the form of other hydrocarbons can also be employed.

(3) *Pumping by a CO_2 laser.* There are many gases that will generate far-infrared radiation when pumped by the CO_2 laser. CO_2 lasers in which the active element is a tube supporting a low-pressure dc discharge can be operated either continuously or as Q-switched devices. In either case, CO_2 lasers can be used to pump lasers working in the far infrared. The stationary discharge current in the low-frequency tube of the CO_2 laser is often modulated by 0.1–0.5-ms current pulses with amplitudes of a few hundred mA.[88] This pulsed-periodic operation results in relatively high peak power in the CO_2 laser and pulse lengths of $\tau \sim 100$–500 μs (in contrast to the Q-switched regime for which $\tau \leqslant 1$ μs).

New opportunities for gas pumping arise when pulsed CO_2 TEA lasers with power levels of 100 kW-10 MW are employed (Ref. 234). Because of the broadening of molecular levels of the gas by the electric field of the pump, it is possible to excite levels that are substantially detuned from the pump frequency.[89] Moreover, it has recently become possible to achieve continuous frequency tuning in pulsed-ionization CO_2 lasers working at a high (up to 10 atm) working gas pressure,[40] which extends the possibilities of the CO_2 laser as the source of pump radiation. Thus, new lines appear in the spectra generated by gases which could not be seen prior to the advent of pulsed TEA lasers. On the other hand, the use of the pulsed CO_2 TEA lasers requires the availability of detectors capable of coping with pulses about 100 ns long.

C. Experimental results on the generation of far-infrared radiation

(1) *Lines generated at present with the aid of optical pumping in the far infrared.* There are now more than 30 materials whose molecules (in the gas phase) can generate more than 800 far-infrared lines when optically pumped. The entire far-infrared range covers just over six octaves between 30 μm and 2000 μm, but the line density at different points in this range is not the same.

Figure 8 shows a histogram of the distribution over

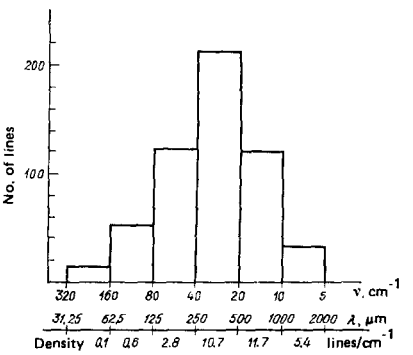

FIG. 8. Histogram of laser-line density in the far-infrared.

the range of the number of lines per octave.[78] The distribution maximum occurs between 20 and 40 cm^{-1} (250–500 μm). The reduction in the number of lines at either end of the infrared range is partly due to the fact that the detectors used at the edges of this distribution have sensitivity "valleys." Moreover, the mirrors of open resonators at the long-wave end of the range may lead to a deterioration in reflectance. There appears to be, however, a physical reason for the distribution shown in Fig. 8.[78] The gain of the far-infrared laser is, roughly speaking, proportional to $\nu_{ij}\Delta n_{ij}$, where $\nu_{ij} = 2Bj$ is the frequency of the generating transition (regarded as a rotational transition), B is the rotational constant, j is the rotational quantum number, and Δn_{ij} is the attainable inverted population which, for a sufficiently strong pump, is determined by the population of the initial state from which the material is pumped. The equilibrium (thermal) distribution of the rotational-level populations must be of the form shown in Fig. 9 and is described by

$$n_j \sim (2j+1)\exp\left(-\frac{E_j}{kT}\right), \tag{4.3}$$

where E_j is the energy of the j-th rotational level at gas temperature T.

This figure also shows ν_{ij} as a function of j, and it is clear that the product $n_j\nu_{ij}$ has a maximum near a certain value of j which we shall represent by j'. We then have $E_j' \sim hBj'^2c \approx kT$, and hence $j' \approx \sqrt{kT/hBc}$ and the frequency of the generating transition at maximum gain is $\nu_{ij} \sim \sqrt{4BkT/ch}$. For many molecules, the constant B lies in the range 0.5–1 cm^{-1}, so that the position of peak gain (and, correspondingly, of maximum line density) occurs in the range 22–32 cm^{-1} when the gas is at temperature $T \sim 300$°K.

Table III lists molecular gases capable of generating far-infrared radiation when they are optically pumped,

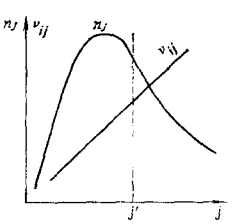

FIG. 9. Level population n_j and transition frequency ν_{ij} as functions of j.

TABLE III. Molecular gases generating far-infrared radiation when optically pumped.

Type of molecule	Molecule	References	Diatomic molecule	Molecule	References
Diatomic molecule	HF	111, 112, 139	Asymmetric top	O_3	96
				D_2O	100, 101, 118–123, 207–211
Symmetric top	CH_3F	88, 90, 113, 114, 121–123		CH_3OH	88, 90, 94, 98, 99, 102–106, 115
	CH_3Cl	90–92		CH_3OD	102, 115
	CH_3Br	92		CD_3OD	107
	CH_3I	92, 93, 110		CH_3CH_2OH	91
	CH_3CN	92, 94, 111		HCOOH	94, 96, 108, 109, 118
	CH_3CCH	114		CH_2OHCH_2OH	108
	CD_3I	116		NH_2NH_2	110
	CD_3Cl	116		CH_3NH_2	94, 98, 108
	CH_3CF_3	50		CH_3CH_2F	94, 96
Symmetric top with inversion	NH_3	88, 90, 95–97–121–123, 125		CH_3CH_2Cl	91
	$^{15}NH_3$	121		CH_3CHF_2	90, 95
				CH_3OCH_3	108
Asymmetric top	CH_2Cl_2	91		HCOOD	118
	CH_2CHCl	88, 94		DCOOH	118
	CH_2CHCN	94		DCOOD	118
	CH_2CF_2	94, 98, 99		CD_3OH	117

together with appropriate references. (An analogous table summarizing the state of the art in the middle of 1976 is given in Ref. 78). Apart from the HF molecule that was excited by the HF laser, and the $^{14}NH_3$ molecule whose two lines were excited by the N_2O laser, all the molecules in Table III were excited by the CO_2 laser. As noted above, the CO_2 laser is the most convenient and the most widely studied source of radiation (both cw and pulsed), and has dominated the subject as a source of pumping radiation for FIR lasers. A list of 120 "strong" laser lines in the far infrared is given in Ref. 78. These lines are generated when the sources are pumped by CO_2 lasers. "Strong" transitions are those capable of producing radiation of 10^{-4} W or more under cw or quasi-cw conditions. This listing is only preliminary because new close coincidences have recently been discovered both for previously known molecules as a result of the use of the CO_2 laser in the second band of the sequence (00°2-02°1 or 00°2-10°1 transitions)[123] and as a result of the introduction of optically pumped molecules containing nontraditional isotopes into the working laser.[124] In earlier work (see Table III), the relative combination of the isotopes H and D was varied in the active molecules.

(2) *The first optically-pumped* CH_3F *laser.* The possibility of making an optically-pumped far-infrared laser was first demonstrated by Chang and Bridges in 1970.[113] The CH_3F molecules were pumped by the P(20) 9.6-μm line of a Q-switched CO_2 laser. In accordance with spectroscopic data available for CH_3F (Ref. 126), pumping in the Q-branch was expected for $j = 12$. By varying the pump frequency within the limits of 50 MHz, it was found possible to excite transitions with $k = 1, 2$ and $j = 12$ in absorption. The result was that, for each value of k, there were three lines generated in the region of $\lambda = 496$ μm, and two in the $v = 1$ band (cascade generation), and one in the $v = 0$ band (depletion of the initial level). The radiated power was about 0.1 W for $p = 0.1$–0.2 Torr. A power level of about 0.5 MW ($p \sim 3$ Torr) was achieved by pumping CH_3F with the pulsed CO_2 TEA laser[105,125–131] when the cell was optically pumped under superradiant conditions (without mirrors). The corresponding linewidth turned out to be greater than 100 MHz, but mode-locking in the CO_2 laser reduced the linewidth down to 30 MHz (Ref. 100). The optically-pumped CH_3F cell has been used in the development of a powerful laser producing a very narrow line and designed for research into Thomson scattering by plasmas in thermonuclear systems.

A system consisting of a master laser and an amplifier, and capable of producing hundreds of kilowatts for a linewidth of about 40–50 MHz, was investigated as part of this program.[132,133]

(3) NH_3 *laser.* Ammonia, NH_3, is one of the gases consisting of symmetric-top molecules and is among the most widely studied in spectroscopy. The relative position of the spectral lines of NH_3 and of the lines generated by the CO_2 and N_2O lasers was investigated in Ref. 134. This enabled Chang *et al.*[95] to develop an NH_3 laser pumped by a cw N_2O laser [$P(13)$ 10.78-μm lines] which produced two far-infrared lines. One of these lines ($\lambda = 81.5$ μm) was the result of the inversion-rotation transition in NH_3, and the other ($\lambda = 263.4$ μm) was due to pure inversion transition with $\Delta j = 0$. Despite the fact that the absorbing transitions from the ground state of NH_3 in the ν_2 band overlap satisfactorily the P and R branches generated by the CO_2 laser, there are no close coincidences ensuring the operation of the optically pumped laser in the cw mode. Nevertheless, the use of a powerful pulsed CO_2 TEA laser[89,90] has resulted in the generation of many transitions in NH_3 because of the broadening of the absorbing transitions by the electric field of the pump. Moreover, by placing the NH_3 cell in a constant electric field, Fetterman *et al.*[97] produced generation on several transitions by using a cw CO_2 laser pump. They noted that the Stark effect led not only to a shift of the absorption lines in NH_3, leaving the generated lines virtually unshifted, but also made the selection rules less stringent in absorption. When gaseous $^{14}NH_3$ and $^{15}NH_3$ are pumped by the cw CO_2 laser operating in the second band of the "sequence"[123,124] (00°2 – 02°1 transition), the external field becomes unnecessary because new close coincidences are found between the pump and absorption frequencies.

(4) CH_3OH *laser.* Methyl alcohol (CH_3OH) is a convenient working medium for the far infrared when a cw or quasi-cw CO_2 laser is used as the pump.[88,80,94] This laser produces a record number of lines (82) in the far infrared, which is due to the asymmetry of the CH_3OH molecule and the presence of a torsional vibration mode of the OH group, which is active in the far infrared.

(5) HF *laser.* The only diatomic molecule generating in the far infrared is HF (Refs. 111, 112). When the pulsed HF laser ($\lambda \sim 2.7$ μm) is used to pump a cell containing gaseous HF (12 cm long), the HF molecules turn out to be in the vibrational-rotational band with $v = 1$ (transition from the ground state). When the gas pressure in the cell is 0.05–6 Torr and the pump power is in the range 3–4 kW, there are seven generated lines with wavelengths between 36.5 μm and 252.7 μm. Since the HF molecule has a large constant dipole moment, and the pump frequency coincides with the frequency of

the absorbing transition, the HF cell is capable of high gain (>1 cm^{-1}), so that the system will operate in the superradiant state.[35] It was found[135] that, when the HF pressure was in the range 0.001–0.02 Torr and the cell length was about 1 m, the superradiant state ensured the emission of far-infrared radiation through both ends of the cell with a delay of 0.5–2 μs relative to the pulse. The superradiant pulse consists of a "first peak" whose length is between 1/4 and 1/2 of the delay relative to the pump and a "ringing" tail. A reduction in pressure or pump power leads to an increase in the delay and in the length of the first peak, and to a reduction in the peak generated power.

(6) D_2O *laser.* The heavy-water molecule appears to be one of the most promising molecules for the generation of powerful pulses of far-infrared radiation when it is pumped by the pulsed CO_2 TEA laser. Although there are no exact coincidences between the D_2O absorption frequencies and the CO_2 laser lines, a strong enough pump (about 100 MW) will give rise to generation in the superradiant mode.[100,101,119-122] As much as 10 MW can be produced in some of the lines[100] (when fast oscillations are averaged on an oscillogram), and the efficiency is about 7%. When the pump is in the form of the $P(32)$, $R(12)$, and $R(22)$ lines in the 9.6-μm band of the CO_2 TEA laser, it is found that powerful lines appear at about 66 μm, 114 μm, and 385 μm, and weaker lines appear at about 117 and 50 μm. When the D_2O laser was pumped in Refs. 207–211 by the 9R(22) line of the CO_2 laser, the 385-μm D_2O-laser radiation was augmented by emission at about 359 μm, whereas 239-μm radiation was observed in Ref. 210. A record combination of the parameters of an optically pumped D_2O cell ($p \sim 3$ Torr) was achieved in Ref. 210 near $\lambda \sim 385$ μm (pulse power 800 kW, linewidth 50 MHz, detuning $\Delta\nu \sim 2$ GHz, energy efficiency 0.4%). We note that the optically pumped D_2O cells used in Refs. 209–211 and, possibly, in Refs. 207, 208, were working both in the laser regime (with population inversion) and in the resonant SRS regime (see below). The use of the CO_2 laser working in the second band of the sequence ($00^\circ2 - 02^\circ1$ transitions) as a pump for the D_2O cell results in close coincidences sufficient for generation in the cw mode.[123]

The superradiant regime can also be achieved in a cell containing NH_3, CH_3CN, CH_3Cl, or CH_3Br and pumped by the CO_2 TEA laser.[100]

(7) *Lasers using resonant* SRS (NH_3, HCl, HF, *and* D_2O). By illuminating the gas with high-power radiation whose wave-length corresponds to the energy of the absorbing transition in the gas, or is close to it, it is possible to achieve not only lasing due to population inversion between any two levels, but also to ensure that the pump radiation (ω_1) gives rise to resonant stimulated Raman scattering (RSRS) with resonant frequency ω_2 (Fig. 10) if the SRS active gas has energy levels (for example, $j+1$ for $v=1$ or $j-1$ for $v=0$ in Fig. 10) such that the pump frequency ω_1 is close to an absorption line j, $v=0 \to j+1$, $v=1$ or $j-1$, $v=0 \to j$, $v=1$ (Refs. 79, 80, and 136).

Even in Ref. 137, in which NH_3 was optically pumped

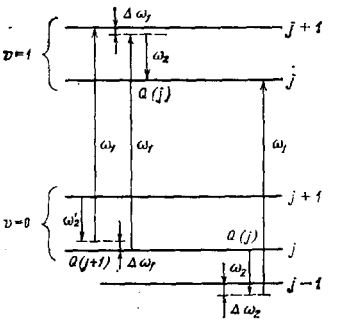

FIG. 10. Partial level scheme for the HF molecule and transitions during RSRS.

by a pulsed CO_2 laser, the spectrum was found to contain lines with frequencies close to the frequencies of transitions for which inversion could not be achieved for realistic gas temperatures because the corresponding levels were too close together. A study was made of lines in the range $\lambda \sim 11$–12 μm. The shift of NH_3 lines from close transition frequencies (that could be radiated) corresponded to a detuning of the pump frequency from the frequency of the absorbing transition in NH_3. At the same time, optical pumping of NH_3 detuned in frequency from the absorbing transition, did not lead to a shift of the generated line from the frequency of the corresponding transition in the far infrared.[89,90]

When different D_2O laser arrangements pumped by the 9.26-μm CO_2 laser radiation were investigated, it was found[207,209-211] that the emission spectrum and the gain of the D_2O laser near $\lambda \sim 385$ μm could be explained only by taking into account both laser generation and RSRS processes. It was noted previously[122] that an increase in the D_2O pressure in an optically-pumped cell should lead to an increase in the contribution of RSRS near $\lambda \sim 385$ μm. For a relatively low pumping level, and precise resonance between the pump frequency and the frequency of the absorbing transition and a low D_2O pressure, emission by the D_2O cell was found[210] to occur via a laser mechanism, while a detuning of the pump frequency from the frequency of the absorbing transition, an increase in the pump power, and an increase in the D_2O pressure led to the predominance of the RSRS mechanism of emission near $\lambda \sim 385$ μm.

There have been recent publications[138,139] in which frequency-tuned ($\Delta\nu \lesssim 5$ cm^{-1}) generation of far-infrared radiation was produced via the RSRS mechanism in HCl and HF (see Fig. 10). The pump (in the R branch of HCl or HF) was a frequency tunable generator ($\lambda \sim 2.5$ μm) based on double SRS in hydrogen of dye-laser radiation.[140] A graph of the detuning of the frequency of the RSRS generator near the frequencies of the corresponding rotational transitions is given in Ref. 139. This graph also shows points corresponding to the operation of an optically-pumped laser that operates only when the pump radiation is detuned from the absorption line of HF. The power generated by the RSRS generator is about 300 kW and the quantum efficiency is about 18%.

Experiments have also been carried out[38,125,141] in which optical pumping of one of the NH_3 levels leads to

the simultaneous generation of several lines (including lines in the far infrared), so that the active molecules finish up in the initial (ground) state. The emission of some of the observed lines[38,141] generated by the optically-pumped laser cannot be explained because it is basically impossible to achieve population inversion for at least one of the sequences of transitions in the active NH_3 molecule. The generation of these series must therefore be explained by assuming that RSRS processes or resonant optical frequency mixing in NH_3 are taking place.

5. ELECTRICAL-DISCHARGE LASERS FOR THE FAR INFRARED

A. Excitation of a gas laser by electrical discharge

Lasers based on transitions in neutral gas atoms can be excited by an electrical discharge whose properties are connected with the way inversion is established for the generating transition. Dc or hf discharges are used to excite cw lasers. A pulsed discharge (with afterglow) can excite pulsed generation in a gas and, finally, lasers based on self-limiting transitions (for which the lower laser level is not depopulated) are excited by a discharge pulse with a steep leading front.

The positive column of a glow discharge in a cylindrical tube is frequently used to pump cw lasers. The positive column of the glow discharge is in the form of a weakly-ionized nonequilibrium plasma with degree of ionization equal to 10^{-6}–10^{-7} and average electron velocity much greater than the gas temperature (about 1–2 eV). The current density in such a discharge is usually 100–200 mA/cm^2. The average electron energy T_e in the positive column is determined from the balance of charged particles produced by the T_e-dependent volume ionization, which vanish as a result of diffusion toward the tube wall on which they recombine. Analysis of processes occurring in the positive discharge column in a pure gas[142] and in a gas mixture[143] has shown that, if the electrons lose their energy mainly as a result of elastic collisions with atoms, the temperature T_e (which depends on the ratio E/p, where E is the electric field and p the gas pressure) is determined by the product pD, where D is the discharge-tube diameter. A reduction in pD is accompanied by an increase in the average electron energy and in the ratio E/p, whereas an increase in pD is accompanied by an increase in the average energy T_e and E/p. The conditions in the discharge are very similar for equal values of pD, and the parameter pD can be used to control the properties of the discharge in order to ensure the best excitation of any given upper laser level.

The generating transition can be excited either selectively or nonselectively in the positive column of the glow discharge. Nonselective pumping by electron impact, either directly or through intermediate levels, will populate the upper and lower levels participating in the generation process at roughly the same rate. Selective pumping is achieved either by electron impact if the populated level is connected to the ground state by an allowed transition (in the dipole approximation) or through resonant transfer of excitation to the upper working level from impurity atoms to the generating atom (from molecule to molecule, respectively).[144,145] In the case of nonresonant pumping, population inversion is produced because the levels are depopulated at different rates.

The gain of the electrical-discharge laser is given by (4.1). In most cases, the gain is difficult to calculate because there is a lack of data on the cross sections for level excitation by electron impact. When the effective excitation cross sections are known as functions of energy, the excitation dynamics and the properties of the discharge can be calculated on a computer, as was first done for the CO_2 laser (working at $\lambda = 10$ μm) in Ref. 146. In any case, an increase in the gain for a given transition is facilitated by (1) an increase in the transition probability, (2) more selective excitation of the upper laser level, and (3) an increase in the difference between the relaxation times of the upper and lower laser levels.

The pulsed discharge was first used in Ref. 147 to excite laser generation by neutral atoms. The current density in pulsed discharges can reach hundreds of amperes per square centimeter.

A pulsed discharge can be produced for different values of the electrode separation: about 1 m in tubes and a few centimeters in lasers with a transverse discharge.[148,186,187]

Depending on the method used to excite the upper laser level (direct or indirect), and the properties of the pulsed discharge, generation will develop together with a current pulse or with a delay relative to this pulse.

The conditions prevailing in a pulsed discharge cannot be characterized by pD alone. They are also found to depend on the type and pressure of gas, on the method whereby energy is transferred from the discharge electrons, on the shapes of the leading and trailing current pulse fronts, and on the electrical parameters of the circuit. As a rule, high gain and high peak emission power can be reached in the pulsed discharge.

B. Far-infrared lasers using transitions in neutral atoms

(1) *The first electrical-discharge laser using* Ne. As far back as 1964, neon transitions pumped by a dc discharge were used to produce generation in the range between 30 and 133 μm (Refs. 149, 150). The generator was a discharge tube, 3–5 m long and 10–25mm in diameter, filled with neon at a pressure of 0.01–0.1 Torr. In some experiments, helium was added to neon in amounts exceeding the amount of neon by a factor of 2–5. High-lying neon levels (principal quantum number $n \sim 6$–9) took part in the generation. An open resonator was employed and the radiation was allowed to escape through coupling apertures in one of the mirrors. A complete list of neon lines (in the middle infrared at about 30 μm) is given in Ref. 151.

(2) He *laser*. Two infrared lines have been found at about 95.8 and 216.3 μm in discharge-excited helium.

The former line was recorded first under pulsed excitation[152] in a tube, 7.5 cm in diameter, at a pressure of 0.5 Torr. Both lines were subsequently generated in a dc helium discharge in a tube, 6 cm in diameter, at a pressure of 0.1 Torr (Ref. 153). The transitions were identified as $3^1P_1 - 3^1D_2$ for the first line, and $4^1P_1 - 4^1D_2$ for the second line. Improved values for the two wavelengths were subsequently obtained[154] by using a pulsed discharge in helium with a current-pulse width at half-height of about 1 μs and current amplitude of 4–18 kA in a tube 2 m long and 15 cm in diameter. Experiments were performed at pressures of about 0.1–0.7 Torr, and a generated pulse of about 0.7 μs was found to appear on the growing part of the current of duration ~1 μs. As noted in Ref. 154, population inversion is possible between the levels participating in the generation process, firstly, as a result of an increase in the lifetimes of the upper laser levels due to the trapping of the resonance radiation that appears as a result of the decay of the upper levels, and, secondly, because of the higher cross section for the excitation of the upper level (by a factor of about 10).

(3) Xe *laser*. The only far-infrared line ($\lambda \simeq 75.6$ μm) was found in xenon when the tube diameter was 0.6 cm and a 100:1 mixture of helium and xenon was used to maintain the continuous discharge[155] at xenon pressure of 0.035 Torr.

C. Lasers for the far infrared using molecular transitions

There are seven known molecular gases that can generate far-infrared radiation when pumped by an electrical discharge ($\lambda \simeq 30$–2000 μm): HCN, H_2O, SO_2, H_2S, OCS, and HBr. HCN and H_2O molecules have three modifications, each of which generates in the far infrared and differs by the presence of different H, N, and O isotopes: HCN, DCN, HCN^{15}, H_2O, D_2O, and H_2O^{18}. One of these molecules is diatomic, another contains four atoms, and the remaining molecules are triatomic.

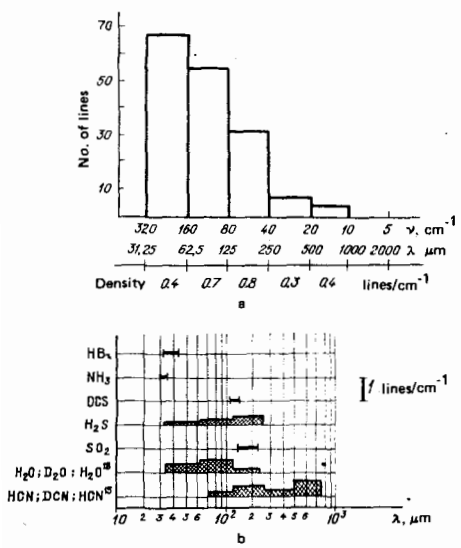

FIG. 11. Histogram of laser-line density in the far-infrared (a), and laser-line density in the far-infrared for different gases (b).

Figure 11a shows a histogram giving the number of lines per octave due to molecular-discharge lasers (the range 5–320 cm^{-1} is divided into six octaves). The lower part of the figure shows the line density (per centimeter) in each of the octaves. Figure 11b shows the wavelength ranges containing the lines generated by these gases. The line distribution densities are different in the different intervals, and the line intensities are also very different. For H_2S, H_2O (together with H_2O^{18} and D_2O), and HCN (together with DCN and HCN^{15}), the intervals containing the generated lines are divided into six octaves, as in Fig. 11a. The height of the black rectangle in each octave represents the number of lines per reciprocal centimeter. The corresponding scale is shown on the right of Fig. 11b. The total number of far-infrared lines generated by discharge lasers containing HBr, OCS, SO_2, NH_3, H_2S, HCN (together with DCN and HCN^{15}), and H_2O (together with D_2O and H_2O^{18}) is 8, 2, 4, 4, 23, ~37, and ~88, respectively. A listing of these lines together with the corresponding frequencies and transition identifications (when available) is given in Ref. 156.

(1) HCN *laser*. Far-infrared radiation was first observed in 1963 in Ref. 157, in which a pulsed discharge in a mixture of molecular gases containing H, C, and N was produced in a glass tube with an optical resonator. This was followed by a number of other publications,[158–161] in which the generation of radiation with $\lambda \sim 337$ μm was investigated and new lines were found when the discharge was produced either in individual gases or in gas mixtures such as $CH_4 + NH_3$, $CH_4 + N_2$, CH_3CN, $(CH_3)_2NH$, HCN, or in mixtures where deuterium replaces hydrogen, for example, $D_2 + BrCN$, $CD_4 + ND_3$. A typical arrangement is a discharge tube (made of glass), 3–6 m long and 5–15 cm in diameter, containing a gas mixture at a pressure of about 0.1–1 Torr. The pulsed voltage between the electrodes is about 15–40 kV and the current per pulse is 200–900 A. The current pulse length is about 10 μs, the generation pulse is longer by a factor of 2–3 than the current tube, and the pulse repetition frequency is usually less than a few hertz. The generated pulse is delayed by about 30 μs relative to the discharge current. The experimental techniques are described in greater detail in Refs. 160 and 161 and in the references therein.

The decisive step toward an understanding of the principle of operation of the laser exploiting a discharge in a mixture of molecular gases containing H, C, and N atoms was made in Ref. 168, where it was pointed out that the observed generation was the result of vibrational-rotational transitions between one of the composite modes (11^1–0) and a harmonic of the deformational mode 04^00) in the linear molecule HCN, produced in the discharge. The probability of these intermediate transitions in HCN under ordinary conditions is too low for the gain necessary for generation to be reached. However, in the case of the 11^10–04^00 transition in the HCN molecule, the higher probability necessary for generation is achieved as a result of a coincidence between energies of some of the rotational components with equal j that belong to the 11^10 and 04^00 levels (Fig. 12). The coincidences between the energies

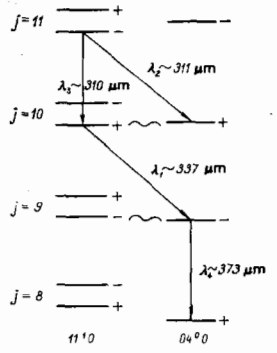

FIG. 12. Part of the vibrational-rotational spectrum of the HCN molecule.

of rotational components lead to the so-called "mixed" quantum states which are good candidates for participation in laser transitions[168] ($\lambda_1 \sim 337$ μm and $\lambda_2 \sim 311$ μm in Fig. 12). The vibrational-rotational intermode transitions, in turn, give rise to pure rotational transitions without a change in the vibrational state of the HCN molecule (for example, $\lambda_3 \sim 310$ μm and $\lambda_4 \sim 373$ μm in Fig. 12), i.e., we have cascade generation.[168,169] The proposed appearance of mixed quantum states[169] has led to the identification of many of the lines generated as a result of discharges in gas mixtures containing H, C and N (D, C, and N) with the 11^10-04^00, 12^20-05^10, and 12^00-05^10 transitions in the HCN molecules, and the $22^00 \rightarrow 09^10$ transition in DCN (plus the group of pure rotational transition due to the cascade mechanism[156]). However, many of the lines generated by the HCN laser and all the lines of the HCN^{15} laser remain unidentified.

As a rule, the peak power emitted in the strongest lines does not exceed 1–10 W (Refs. 156, 162, 163, and 160) but, nevertheless, the authors of Ref. 164 succeeded in reaching a peak power approaching 1 kW with the HCN laser at $\lambda \sim 337$ μm. Some of the lines produced by HCN and DCN lasers are generated in the cw mode[165–167] when a dc or hf discharge is maintained in the discharge tube. The gain of the HCN laser is usually about 70% per meter under pulsed excitation, and about 10% per meter in the stationary discharge.[170]

(2) H_2O *laser*. Laser emission from a pulsed discharge in a tube containing H_2O vapor was first reported in 1964.[171] The tube had a diameter of 2.5 cm and was 4.8 m long. It was equipped with an aluminized mirror at one end and a flat polyethylene or silicon window at the other. A pulsed discharge was excited in the H_2O vapor (about 1 Torr) with a current pulse length of about 3 μs and a potential difference between the electrodes of about 46 kV. It was found that generation could be detected in the range 23–79 μm, with six lines lying in the range 30 μm $< \lambda <$ 2000 μm. Between one and ten watts were generated in three out of the six lines, and 1 W was produced in the remaining lines. Pulsed generation in a discharge tube containing D_2O vapor[172] was also achieved in 1964. This was followed by further publications, reporting new laser lines from H_2O and D_2O vapor, and studies were carried out of the properties of the radiation emitted by such lasers.[173–178] A total of 46 lines was recorded in the far infrared in the case of the H_2O laser, but 15 of these were not confirmed by subsequent research (see Ref. 156). The H_2O^{18} laser generates 7 lines in this range, and the D_2O laser 35 lines (7 of these have not been confirmed). Many of the H_2O and D_2O laser lines are generated in the cw mode:[179,180] 10 lines in H_2O and 4 lines in D_2O. The experimental techniques for pulsed FIR generation in water vapor are essentially analogous to the equipment described in connection with the HCN laser. The tube containing the H_2O vapor at a pressure of about 1 Torr was excited by a pulsed discharge using a current of a few amperes at 15–45 kV. Its length was 3–5 m and the diameter was 2.5–10 cm. One of the pair of mirrors used in the resonator at the ends of the tube was always metallized and completely reflected electromagnetic radiation, whilst the other was prepared from a material that was semitransparent or had an aperture to allow the power to escape from the cavity. The current pulse length was usually a few microseconds, and the length of the generated pulse was 1.5–50 μs under typical conditions (depending on the particular line). The delay time and length of the generated pulse were determined by the processes responsible for population inversion in the corresponding transition.[174] However, for discharge current pulses of about 500 μs (about 2–10 A), some of the lines[178] were found to be generated for about 50–150 μs and the generation was delayed by up to 100 μs. The pulse repetition frequency was up to 500 Hz and the working gas was allowed to flow through the tube in order to remove heat from the working region. More detailed information on the design and properties of H_2O lasers with pulsed excitation can be found in Ref. 181 and in the references given therein. The experimental techniques used for continuous-wave generation of the far infrared in H_2O is the same as that used for the pulsed systems.[179,180]

The $H_2O(D_2)$ molecule is a nonlinear, polar molecule. The position of the energy levels corresponding to the lower vibrational states of H_2O has been known for a relatively long period of time. It has also been known for a long time that the excitation of the bending mode of H_2O relaxes much more rapidly than the symmetric or antisymmetric mode, so that inversion of populations in $(v00) \rightarrow (0v0)$ or $(00v) \rightarrow (0v0)$ transitions can arise even under nonselective pumping. However, the observed lines generated in the water molecule could be interpreted in terms of $(100) \rightarrow (020)$ and $(001) \rightarrow (020)$ transitions and the associated purely rotational transitions (cascade generation) only after the emergence of the concept of mixed states,[168] involving pairs of levels belonging to different vibrational modes (as was the case in HCN). A partial energy-level scheme is shown in Ref. 156 for H_2O and D_2O, together with the identification of most of the laser transitions that have been recorded.

The pulsed power generated by the H_2O laser is very different for different lines[156] and may reach 10 W in the case of the strongest lines. The peak power in the weaker lines is about 0.001 W. The power output of the D_2O laser does not usually exceed 1 W, and that of the H_2O^{18} laser does not exceed 0.01 W. A record power of about 5 kW was achieved in Refs. 182 and 183 as a re-

sult of the optimization of the H_2O laser parameters at $\lambda \sim 28$ μm (superradiant line),[179] but this line lies outside the range considered here.

The generation of far-infrared radiation by a pulsed discharge in HCN and H_2O has been characterized by the so-called longitudinal excitation scheme in which the discharge current flows along the axis of the discharge tube, which coincides with the optical axis of the resonator.

(3) HCN *and* H_2O TE *lasers*. The success of the transverse discharge in which the current flows at right-angles to the optic axis is well known in relation to the pulsed gas-discharge CO_2 laser working at atmospheric pressure (the TEA laser),[148] and this has stimulated attempts to extend the TEA method to other gases.[184] Among the molecules capable of generating far-infrared radiation in an electrical discharge, H_2O was found to generate several lines in a transverse discharge at 45 Torr,[184] of which only the $\lambda \sim 28$ μm line was classified as "strong." However, even this strong line was not stronger than for lasers with a longitudinal discharge. It is noted in Ref. 185 that there is little prospect of increasing the power that can be produced under pulsed generation by using a short ($\lesssim 1$ μs) transverse discharge at higher pressure, at least for HCN, SO_2, and H_2S. This is said to be due to the fact that the upper laser levels of HCN, SO_2, and H_2S are not directly excited by electron impact in the discharge. This is indicated in particular by the fact that the HCN, SO_2, and H_2S laser pulses appear after an interval of a few tens of microseconds after the current pulse. On the other hand, when the H_2O laser operates at about 28 μm, the generated pulse appears practically simultaneously with the current, so that it is assumed that the upper laser level is excited directly by electron impact. It is important to note that some of the H_2O laser lines can also be delayed relative to the current.[172]

(4) HCN *waveguide laser*. The transverse discharge has been successfully used[188] to excite the HCN laser operating at $\lambda \sim 337$ μm. The discharge zone was about 4 m long and in the form of a rectangular waveguide (5 cm$\times$5.8 cm) with one metal wall (anode) and three dielectric walls. The separation between the anode and the dielectric wall supporting the cathode elements in the form of wire inserts (diameters about 0.5–1 mm) was 5 cm. Metal mirrors were mounted at the ends of the waveguide discharge zone, and the radiation was extracted through mylar film mounted in the resonator at an angle to its axis. It was considered in Ref. 186 that the output power of lasers using transverse discharge was restricted by the fact that the structure of the electromagnetic field in the resonator was disturbed by the elements of the discharge chambers in the TEA-type laser.

The waveguide design of the discharge zone proposed in Ref. 186 is free from this defect and can be used to increase the HCN laser output by "two orders of magnitude as compared with previous values"[186] (this, of course, refers to output powers of the order of a few tens of kilowatts). There was no delay between the current pulse and the generation pulse in Ref. 186.

A pulsed HCN laser with transverse excitation and preionization by ultraviolet radiation has also been reported.[187] The energy per pulse was between 1 and 15 mJ when an HCN + CH_4 + He mixture was employed. The discharge chamber had waveguide properties for the emission of far-infrared radiation.

(5) NH_3 *laser*. The FIR generation in a pulsed discharge in NH_3 was first reported in Ref. 188 in 1965 and subsequently in Ref. 189. The discharge tube used in the former experiments had a diameter of 5 cm and a length of 7 m. The gas pressure was 2.4 Torr and the pulse repetition frequency 1 Hz. In Ref. 189, the diameter of the discharge tube was 10 cm, its length was about 5 m, and the current per pulse was 600 A at a gas pressure of 0.5–1.0 Torr. A total of 4 lines was recorded (30.69, 31.47, 31.95, and 32.13 μm). One of the NH_3 lines was not identified although some of the shorter-wavelength lines were given preliminary assignments in Ref. 190.

(6) SO_2 *laser*. Two of the far-infrared lines generated in the SO_2 discharge ($\lambda \sim 141$ μm and $\lambda \sim 193$ μm) were first reported in Ref. 191 for a dc discharge (0.15 A) in a tube, 2.5 m long with an internal diameter of 5.6 cm. The buffer gas was helium at a pressure of 1.5 Torr (SO_2 pressure 2.1 Torr). The same two lines were seen in a dc discharge in Ref. 192. All four lines ($\lambda \sim 141$ μm, $\lambda \sim 151$ μm, $\lambda \sim 193$ μm, and $\lambda \sim 215$ μm) were seen in Ref. 192 in a pulsed discharge in the SO_2 + He mixture (0.4 + 0.4 Torr). The diameter of the discharge tube was 7.6 cm and its length was 2 m. A current pulse of 90 A was employed at a pulse repetition frequency of 13 Hz. Pulse generation of the 151- and 215-μm lines in a discharge in SO_2 was observed in Ref. 193, when He, N_2, or O_2 was added as the buffer gas. All four lines were identified as transitions in the $001 - 020$ band.[194]

(7) *OCS and* H_2S *lasers*. The two lines generated by pulsed discharge in OCS ($\lambda \sim 123$ μm and $\lambda \sim 132$ μm) and all the 23 lines generated by a pulsed discharge in H_2S belong to the far infrared.[192] None of these lines (from OCS and H_2S) has been identified. The associated transitions have been seen in impurity-free H_2S (and in pure OCS, or with N_2, He, or CO as the buffer gas). The pulse generated by the H_2S laser was 20–100 μs long and was delayed relative to the current by about 20–30 μs when the gas pressure in the tube was about 0.15 Torr. The power generated by the H_2S laser in any of these lines was determined against the H_2S-laser line which produced the same power as the H_2S laser in the same experimental setup. The frequencies of all the H_2S lines are given in Ref. 156 with an indication of the relative line intensity.

(8) HBr *laser*. Eight lines generated by this laser with wavelengths between 30 and 41 μm were found in Ref. 195 in a pulsed discharge produced in a tube containing a mixture of BBr_3 (0.05–0.2 Torr) and H_2O. The lines were identified as due to pure rotational transitions with $v = 0$ (2 lines), $v = 1$ (3 lines) and $v = 2$ (3 lines) in the HBr molecule produced in the discharge. The frequencies and identifications of the HBr laser lines are given in Ref. 156.

6. CONCLUSIONS

The last decade has thus seen pulsed and continuously operating laser sources of radiation, covering the entire far-infrared range between 50 and 1000 μm.

The most promising of these are the optically pumped lasers (their quantum efficiency amounts to a few tens of percent, and the number of generated lines will increase in the future) and sources based on resonant SRS that are capable of continuous tuning at high efficiency (tens of percent in the number of photons).

In addition to the purely physical studies mentioned in the Introduction, far-infrared radiation may find applications in molecular biology, where it may be used to investigate the motion of large molecules (proteins, nucleic acids, phospholipids), membranes, and more complex structures. This refers, in particular, to lyotropic lamellar structures characterized by a spatial periodicity with $d \sim 100$ Å. Such systems should be capable of supporting collective vibrations with frequency $\nu \sim S/d$ (S is of the order of the velocity of sound) lying in the far infrared.

A possible technological application of the far infrared involves the use of this radiation to produce images of objects that are not amenable to direct observation (for example, objects covered by a dielectric screen, so that they cannot be seen in visible or near-infrared radiation).

It is hoped that the exploitation of far-infrared radiation will lead in the next few years to the development of image-forming systems for industry (nondestructive testing), medicine (for example, photographs of wounds under dressings and detection of water retention), and elsewhere.[2]

[1]J.-F. Moser, H. Steffen, and F. K. Kneubühl, Helv. Phys. Acta 41, 607 (1968).
[2]T. S. Hartwick *et al.*, Appl. Opt. 15, 1919 (1976).
[3]J. Mink *et al.*, Spectrochim. Acta, Ser. A 36, 151 (1980).
[4]A. Borg *et al.*, *ibid.* 36, 119 (1980).
[5]D. Miernik and B. B. Kedzia, Bull. Acad. pol. Sci. and Sev. Sci. Chim. 27, 465 (1979).
[6]J. Mol. Spectrosc. 79, 345 (1980).
[7]L. M. Suslikov, V. S. Gerasimenko, and V. Yu. Slivka, Opt. Spectrosk. 48, 789 (1980) [Opt. Spectrosc. (USSR) 48, 436 (1980)].
[8]T. Okada, K. Muraoka, and M. Akazaki, Kakuyugo Kenkyu (in Japanese) 43, 169 (1980).
[9]N. Bloembergen, Nonlinear Optics, Benjamin, N. Y., 1965 [Russ. Transl. Mir, M., 1966].
[10]F. Zernike and J. E. Midwinter, Applied Nonlinear Optics: Basics and Applications, J. Wiley, N.Y., 1973 [Russ. Transl., Mir, M., 1976].
[11]D. W. Faries, K. A. Gehking, P. L. Richards, and Y. R. Shen, Phys. Rev. 180, 363 (1969).
[12]T. Yajima and K. Inoue, Phys. Lett. A 26, 281 (1968).
[13]F. Zernike and P. R. Berman, Phys. Rev. Lett. 15, 999 (1965).
[14]K. H. Yang, A. M. Morris, P. L. Richards and Y. R. Shen, Appl. Phys. Lett. 23, 669 (1973).
[15]D. N. Auston, A. M. Glass, and P. Le Fur, *ibid.*, p. 47.
[16]A. N. Bobrovskiĭ, G. D. Myl'nikov, and D. N. Sobolenko, Kvantovaya Elektron. (Moscow) 5, 444 (1978) [Sov. J. Quantum Electron. 8, 261 (1978)].
[17]V. T. Nguyen and C. K. N. Patel, Phys. Rev. Lett. 22, 463 (1969).
[18]C. K. N. Patel and V. T. Nguyen, Appl. Phys. Lett. 15, 189 (1969).
[19]F. Zernike, Phys. Rev. Lett. 22, 931 (1969).
[20]F. Zernike, Bull. Am. Phys. Soc. 12, 687 (1967).
[21]G. D. Boyd, T. J. Bridges, C. K. N. Patel, and E. Bucher, Appl. Phys. Lett. 21, 553 (1972).
[22]T. J. Bridges and A. R. Strnad, *ibid.*, 20, 382 (1972).
[23]T. Y. Chang, V. T. Nguyen, and C. K. N. Patel, *ibid.* 13, 357 (1968).
[24]R. L. Aggarwal, B. Lax, and G. Favrot, *ibid.*, 22, 329 (1973).
[25]B. Lax and R. L. Aggarwal, Microwave J. 11, 31 (1974).
[26]T. J. Bridges and T. Y. Chang, Phys. Rev. Lett. 22, 811 (1969).
[27]R. L. Aggarwal, B. Lax, H. F. Fetterman, P. E. Tannenwald, and B. J. Clifton, J. Appl. Phys. 45, 3972 (1974).
[28]B. Lax, R. L. Aggarwal, and G. Favrot, Appl. Phys. Lett. 23, 679 (1973).
[29]A. A. Vedenov, G. D. Mylnikov, V. A. Roslyakov, D. N. Sobolenko, and A. N. Starostin, Phys. Lett. A 54, 79 (1974).
[30]A. A. Vedenov, G. D. Myl'nikov, and D. N. Sobolenko, Kvantovaya Elektron. (Moscow) 3, 777 (1976) [Sov. J. Quantum Electron. 6, 424 (1976)].
[31]N. Lee, B. Lax, and R. L. Aggarwal, Opt. Commun. 11, 339 (1974).
[32]N. Lee, B. Lax, and R. L. Aggarwal, *ibid.* 18, 50 (1976).
[33]V. T. Nuygen and T. J. Bridges, Appl. Phys. Lett. 26, 452 (1975).
[34]T. Yajima and N. Takeuchi, Jpn. J. Appl. Phys. 9, 1361 (1970).
[35]V. I. Bogatkin, G. D. Lobov, and V. V. Shtykov, V kn. Kvant. elektron. (in: Quantum Electronics) [in Russian], No. 7(17), Naukova Dumka, 1973, p. 129.
[36]R. L. Aggarwal and B. Lax, in: Nonlinear Infrared Generation, ed. by Y. R. Shen, Springer-Verlag, Berlin, Heidelberg, New York, 1977, p. 19 (Topics in Applied Physics, Vol. 16).
[37]V. T. Nguyen and T. J. Bridges, Phys. Rev. Lett. 29, 359 (1972).
[38]A. N. Bobrovskiĭ, A. A. Vedenov, A. V. Kozhevnikov, and D. N. Sobolenko, V kn. Tezisy dokladov na II Vsesoyuznoĭ konferentsii "Optika lazerov," (in: Abstracts of Papers read to the Second All-Union Conference on "Lasser Optics") [in Russian], Leningrad, 1979, p. 113.
[39]Y. T. Chang, Opt. Commun. 2, 77 (1970).
[40]V. N. Bagratashvili, I. N. Knyazev, and V. V. Lobko, Kvantovaya Elektron. (Moscow) 3, 1011 (1976) [Sov. J. Quantum Electron. 6, 541 (1976)].
[41]C. J. Johnson, G. H. Sherman, and R. Weil, Appl. Opt. 8, 1667 (1969).
[42]R. H. Stolen, Appl. Phys. Lett. 15, 74 (1969).
[43]R. H. Stolen, Phys. Rev. 11, 767 (1975).
[44]C. J. Johnson, G. H. Sherman, and H. Weil, Appl. Opt. 8, 1767 (1973).
[45]H. Poulet and J. P. Mathieu, Vibrational Spectra and Symmetry of Crystals, Gordon and Breach, Paris, 1970 [Russ. Transl., Mir, M., 1973].
[46]V. V. Likhanskiĭ, G. D. Myl'nikov, A. P. Napartovich, A. F. Semerok, and D. N. Sobolenko, Kvantovaya Elektron. (USSR) 5, 897 (1978) [Sov. J. Quantum Electron. 8, 512 (1978)].
[47]T. Yajima and K. Inoue, IEEE J. Quantum Electron. QE-5, 140 (1969).
[48]J. R. Morris and Y. R. Shen, Phys. Rev. A 15, 1143 (1977).
[49]A. Koster and A. Vossoughi, J. Phys. E 9, 340 (1976).
[50]K. H. Yang, P. L. Richards, and Y. R. Shen, Appl. Phys. Lett. 19, 385 (1971).
[51]T. Yajima and N. Takeuchi, Jpn. J. Appl. Phys. 10, 907 (1971).

[52]D. W. Faries, P. L. Richards, Y. R. Shen, and K. H. Yang, Phys. Rev. **133**, 2148 (1971).
[53]T. L. Brown and P. A. Wolff, Phys. Rev. Lett. **29**, 362 (1972).
[54]A. A. Vedenov, G. D. Myl'nikov, V. A. Roslyakov, D. N. Sobolenko, and A. N. Starostin, V kn. Tezisy dokladov, predstavlennykh na VII Vsesoyuznuyu konferentsiyu po kogerentnoĭ i nelineinoĭ optike (in: Abstracts of Papers read to the Seventh All-Union Conference on Coherent and Nonlinear Optics) [in Russian], Moscow State University, 1972, p. 453.
[55]V. A. Roslyakov and A. N. Starostin, Zh. Eksp. Teor. Fiz. **73**, 1747 (1977) [Sov. Phys. JETP **46**, 917 (1977)].
[56]Y. Yacoby, R. L. Aggarwal, and B. Lax, J. Appl. Phys. **44**, 3180 (1973).
[57]A. Yariv, Kvantovaya elektronika i nelineĭnaya optika (Quantum Electronics and Nonlinear Optics) [in Russian], Sovetskoe Radio, M., 1973.
[58]T. Fischer and L. A. Kulevskiĭ, Kvantovaya Elektron. (Moscow) **4**, 245 (1977) [Sov. J. Quantum Electron. **7**, 135 (1977)].
[59]G. P. Arnold and R. G. Wensel, Appl. Opt. **16**, 809 (1977).
[60]R. London, Proc. Phys. Soc. London **82**, 393 (1963).
[61]C. H. Henry and C. G. Garret, Phys. Rev. **171**, 1058 (1968).
[62]V. V. Obukhovskiĭ and V. L. Strizhevskiĭ, V. kn. Kvant. elektron. (in: Quantum Electronics), No. 9 [in Russian], Naukova Dumka, Kiev, 1975, p. 51.
[63]J. M. Yarborough, S. S. Sussman, H. E. Puthoff, R. H. Rantell, and B. C. Johnson, Appl. Phys. Lett. **15**, 102 1969.
[64]B. C. Johnson, H. E. Puthoff, J. Soo Hoo, and S. S. Sussman, *ibid.* **18**, 181 (1971).
[65]M. A. Piestrup, R. N. Fleming, and R. H. Pantell, *ibid.* **26**, 418 (1975).
[66]I. M. Aref'ev, S. V. Krivokhizha, Yu. I. Kyzylasov, V. S. Starunov, and I. L. Fabelinskiĭ, Pis'ma Zh. Eksp. Teor. Fiz. **8**, 142 (1968) [JETP Lett. **8**, 84 (1968)].
[67]V. A. Mishchenko, G. D. Myl'nikov, and D. N. Sobolenko, V kn. Tezisy dokladov Vsesoyuznogo simpoziuma po priboram, tekhnike i rasprostraneniyu millimetrovykh i submillimetrovykh voln (Abstracts of Papers read to an All-Union Symposium on Instrumentation, Technology and Propagation of Millimeter and Submillimeter Waves) [in Russian], Moscow, 1976, p. 27.
[68]V. A. Orlov, Yu. N. Fomin, S. I. Marennikov, and A. I. Parkhomenko, Kvantovaya Elektron (Moscow) **5**, 1808 (1978) [Sov. J. Quantum Electron. **8**, 1026 (1978)].
[69]V. A. Mishchenko, G. D. Myl'nikov, and D. N. Sobolenko, *ibid.* 6, 146 (1979) [Sov. J. Quantum Electron. **9**, 80 (1979)].
[70]M. Born and K. Huang, Dynamical Theory of Crystal Lattices, Oxford University Press, 1954 [Russ. Transl., IL, M., 1958].
[71]D. N. Nikogosyan, Kvantovaya Elektron. (Moscow) **4**, 5, 1977) [Sov. J. Quantum Electron **7**, 1 (1977)].
[72]J. Gelbwachs, R. H. Pantell, E. H. Puthoff, and J. M. Yarborough, Appl. Phys. Lett. **14**, 258 (1969).
[73]E. D. Shaw, Bull. Am. Phys. Soc. **21**, 224 (1976).
[74]J. A. Weiss and L. G. Goldberg, Appl. Phys. Lett. **24**, 389 (1974).
[75]T. Y. Chang, IEEE Trans. Microwave Theory Tech. **MTT-22**, 983 (1974).
[76]N. Bloembergen, Phys. Rev. **104**, 324 (1956).
[77]J. P. Gordon, in: Laser Technology and Application, ed. by S. L. Marshall, McGraw-Hill, N.Y., 1968, p. 31.
[78]T. Y. Chang, see Ref. 36, p. 215.
[79]Q. Javan, Phys. Rev. **107**, 1579 (1957).
[80]P. W. Anderson, J. Appl. Phys. **28**, 1049 (1957).
[81]C. H. Townes and A. L. Shawlow, Microwave Spectroscopy, McGraw-Hill, N.Y., 1955.
[82]J. M. Dowling, J. Mol. Spectrosc. **27**, 527 (1968).
[83]J. S. Garing, H. H. Nielsen, and K. N. Rao, *ibid.* **3**, 496 (1959).
[84]H. M. Mould, W. C. Price, and G. R. Wilkinson, Spectrochim. Acta **15**, 313 (1959).
[85]E. J. Danielewicz, T. K. Plant, and T. A. De Temple, Opt. Commun. **13**, 366 (1975).
[86]D. T. Hodges and T. S. Hartwick, Appl. Phys. Lett. **23**, 252 (1973).
[87]T. Y. Chang and C. Lin, J. Opt. Soc. Am. **66**, 362 (1976).
[88]T. Y. Chang, T. J. Bridges, and E. G. Burkhardt, Appl. Phys. Lett. **17**, 249 (1970).
[89]K. Gullberg, B. Hartmann, and B. Kleman, Phys. Scripta **18**, 177 (1973).
[90]H. R. Fetterman, H. R. Schlossberg, and J. Waldman, Opt. Commun. 6, 156 (1972).
[91]D. A. Jennings, K. M. Evenson, and J. J. Jimenez, IEEE J. Quantum Electron. **QE-11**, 637 (1975).
[92]T. Y. Chang and J. D. McGee, *ibid.* **QE-12**, 62 (1976).
[93]S. F. Dyubko, V. A. Svich, and L. D. Fesenko, Opt. Spectrosk. **37**, 208 (1974) [Opt. Spectrosc. (USSR) **37**, 118 (1974)].
[94]H. E. Radford, IEEE J. Quantum Electron. **QE-11**, 213 (1975).
[95]T. Y. Chang, T. J. Bridges, and E. G. Burkhardt, Appl. Phys. Lett. **17**, 357 (1970).
[96]R. J. Wagner, A. J. Zelano, and L. H. Ngai, Opt. Commun. **8**, 46 (1973).
[97]H. R. Fetterman, H. R. Schlossberg, and C. D. Parker, Appl. Phys. Lett. **23**, 684 (1973).
[98]S. F. Dyubko, V. A. Svich, and L. D. Fesenko, Pis'ma Zh. Eksp. Teor. Fiz. **16**, 592 (1972) [JETP Lett. **16**, 418 (1972)].
[99]D. T. Hodges, R. D. Reel, and D. H. Barker, IEEE J. Quantum Electron. **QE-9**, 1159 (1973).
[100]T. K. Plant, L. A. Newman, E. J. Danielewicz, T. A. De Temple, and P. D. Coleman, IEEE Trans. Microwave Theory Tech. MTT-22, 988 (1974).
[101]F. Keilmann, R. L. Sheffield, J. R. R. Leite, M. S. Field, and A. Javan, Appl. Phys. Lett. **26**, 19 (1975).
[102]S. F. Dyubko, V. A. Svich, and L. D. Fesenko, Zh. Tekh. Fiz. **43**, 1772 (1973) [Sov. Phys. Tech. Phys. **18**, 1121 (1973)].
[103]Yu. S. Domnin, V. M. Tatarenkov, and P. S. Shumyatskiĭ, Kvantovaya Elektron. **1**, 703 (1974) [Sov. J. Quantum Electron. **4**, 401 (1974)].
[104]A. Tanaka, A. Tanimoto, N. Murata, M. Yamanaka, and H. Yoshinaga, Jpn. J. Appl. Phys. **13**, 1491 (1974).
[105]J. R. Jzatta, B. L. Bean, and G. F. Caudle, Opt. Commun. **14**, 385 (1975).
[106]A. Tanaka, M. Yamanaka, and H. Yano, and H. Hirose, Jpn. J. Appl. Phys. **14**, 731 (1975).
[107]S. Kon, E. Hagiwara, T. Yano, and H. Hirose, Jpn. J. Appl. Phys. **14**, 731 (1975).
[108]T. K. Plant, P. D. Coleman, and T. A. De Temple, IEEE J. Quantum Electron. **QE-9**, 962 (1973).
[109]S. F. Dyubko, V. A. Svich, and L. D. Fesenko, Kvantovaya Elektron. (Moscow) No. 5(17), 128 (1973) [Sov. J. Quantum Electron. **3**, 446 (1974)].
[110]S. F. Dyubko, V. A. Svich, and L. D. Fesenko, Zh. Prikl. Spektrosk. **20**, 718 (1974).
[111]N. Kribanowitz, J. P. Herman, R. M. Osgood, M. S. Feld, Jr., and A. Javan, Appl. Phys. Lett. **20**, 408 (1972).
[112]I. P. Herman, J. C. McGillivray, N. Skribanowitz, and M. S. Feld, in: Laser Spectroscopy, ed. by R. G. Brewer and A. Mooradian, Plenum Press, N.Y., 1974, p. 379.
[113]T. Y. Chang and T. J. Bridges, Opt. Commun. **1**, 423 (1970).
[114]T. Y. Chang and J. D. McGee, Appl. Phys. Lett. **19**, 103 (1971).
[115]S. Kon, T. Yano, E. Hagiwara, and H. Hirose, Jpn. J. Appl. Phys. **14**, 1861 (1975).
[116]S. F. Dyubko, L. D. Fesenko, O. I. Baskakov, and V. A. Svich, Zh. Prikl. Spektrosk. **23**, 317 (1975).
[117]S. F. Dyubko, V. A. Svich, and L. D. Fesenko, Izv. Vyssh. Uchebn. Zaved. Radiofiz. **18**, 1434 (1975).
[118]S. F. Dyubko, V. A. Svich, and L. D. Fesenko, Zh. Tekh.

Fiz. 45, 2458 (1975) [Sov. Phys. Tech. Phys. 20, 1536 (1975)].
[119]D. E. Evans, W. A. Peebles, L. E. Sharp, and G. Taylor, Opt. Commun. 18, 479 (1976).
[120]D. E. Evans, R. A. Guinee, D. A. Huckridge, and G. Taylor, *ibid.* 22, 337 (1977).
[121]K. S. Lipton and J. P. Nicholson, *ibid.* 24, 321 (1978).
[122]J. D. Wiggins, Z. Drozdowicz, and R. J. Temkin, IEEE J. Quantum Electron. QE-14, 23 (1978).
[123]E. J. Danielewicz and C. O. Weiss, Opt. Commun. 27, 98 (1978).
[124]E. J. Danielewicz and C. O. Weiss, IEEE J. Quantum Electron. QE-14, 222 (1978).
[125]T. Yoshida, N. Yamabayashi, K. Miyazaki, and K. Eujisawa, Opt. Commun. 26, 410 (1978).
[126]T. Y. Chang, C. H. Wang, and P. K. Cheo, Appl. Phys. Lett. 15, 157 (1969).
[127]F. Brown, E. Silver, C. E. Chase, K. J. Button, and B. Lax, IEEE J. Quantum Electron. QE-8, 499 (1972).
[128]T. A. De Temple, T. K. Plant, and P. D. Coleman, Appl. Phys. Lett. 22, 644 (1973).
[129]F. Brown, S. Kronheim, and E. Silver, *ibid.* 25, 394 (1974).
[130]D. E. Evans, L. E. Sharp, B. W. James, and W. A. Peebles, *ibid.* 26, 630 (1975).
[131]R. J. Temkin, D. R. Cohn, and Z. Drozdowicz, Opt. Commun. 14, 314 (1975).
[132]A. Semet and N. C. Luhmann, Jr., Appl. Phys. Lett. 28, 659 (1976).
[133]D. E. Evans, L. E. Sharp, W. A. Peebles, and G. Taylor, Opt. Commun. 18, 9 (1976).
[134]F. Shimizu, J. Chem. Phys. 52, 3572 (1970).
[135]N. Skribanowitz, J. P. Herman, J. C. McGillivray, and M. S. Feld, Phys. Rev. Lett. 30, 309 (1973).
[136]A. M. Clogston, J. Phys. Chem. Solids 4, 271 (1958).
[137]T. Y. Chang and J. D. McGee, Appl. Phys. Lett. 29, 725 (1976).
[138]R. Frey, F. Pradere, and J. Ducuing, Opt. Commun. 23, 65 (1977).
[139]A. De Martino, R. Frey, and F. Pradere, *ibid.* 27, 262 (1978).
[140]M. Bierry, R. Frey, and F. Pradere, Rev. Sci. Instrum. 48, 737 (1977).
[141]A. N. Bobrovskiĭ, A. A. Vedenov, A. V. Kozhevnikov, and D. N. Sobolenko, Pis'ma Zh. Eksp. Teor. Fiz. 29, 589 (1979) [JETP Lett. 29, 536 (1979)].
[142]A. von Engel and N. Steenbeck, in: Elektrische Gasentladungen, Springer-Verlag, Berlin, Vol. 2, p. 85.
[143]H. B. Dorgela, H. Alting, and J. Boers, Physic Haad. 2, 959 (1935).
[144]C. R. Jones and W. W. Robertson, Bull. Am. Phys. Soc. 13, 198, 1968.
[145]A. V. Eletskiĭ and B. M. Smirnov, Gazovye lazery (Gas Lasers) [in Russian], Atomizdat, M., 1971.
[146]N. L. Nighan, Phys. Rev. A 2, 1989 (1970).
[147]H. A. H. Boot, D. M. Clunie, and R. S. A. Thorn, Nature 198, 773 (1963).
[148]Spravochnik po lazeram (Laser Handbook) [in Russian], Vol. 1, Sovetskoe Radio, M., 1978, p. 133.
[149]W. L. Faust, R. A. McFarlane, C. J. N. Patel, and C. G. B. Garrett, Phys. Rev. A 133, 1476 (1964).
[150]C. K. N. Patel, W. L. Faust, R. A. McFarlane, and C. G. B. Garrett, TIIER, 52, 756 (1964) [Proc. IEEE 52, 713 (June 1964)].
[151]Handbook cited in Ref. 148, p. 11.
[152]L. E. S. Mathias, A. Crocker, and M. S. Wills, IEEE J. Quantum Electron. QE-3, 170 (1967).
[153]J. S. Levine and A. Javan, Appl. Phys. Lett. 14, 348 (1969).
[154]R. Turner and R. A. Murphy, Infrared Phys. 16, 197 (1976).
[155]Yu. N. Petrov and A. M. Prokhorov, Pis'ma Zh. Eksp. Teor. Fiz. 1, 39 (1965) [JETP Lett. 1, 24 (1965)].
[156]Handbook cited in Ref. 148, p. 108.
[157]L. E. S. Mathias and J. T. Parker, Appl. Phys. Lett. 3, 16 (1963).
[158]H. A. Gebbie, N. W. B. Stone, and F. D. Finlay, Nature, 202, 685 (1964).
[159]L. E. S. Mathias, A. Crocker, and M. S. Wills, Electron. Lett. 1, 45 (1965).
[160]L. E. S. Mathias, A. Crocker, and M. S. Wills, IEEE J. Quantum Electron. QE-4, 205 (1968).
[161]H. Steffen and F. K. Kneubübl, *ibid.*, p. 992.
[162]R. Turner and T. O. Poehler, J. Appl. Phys. 39, 5726, 1968.
[163]F. Grams, C. Allen, M. Wang, K. Button, and L. Rubin, Proc. IEEE 55, 420 (1967).
[164]L. E. Sharp and A. T. Wetherell, Appl. Opt. 11, 1737 (1972).
[165]G. T. Flesher and W. M. Mueller, Proc. IEEE 54, 543 (1966).
[166]L. O. Hocker and A. Javan, Phys. Lett. A 25, 489 (1967).
[167]L. O. Hocker and A. Javan, Appl. Phys. Lett. 12, 124 (1968).
[168]D. R. Lide Jr. and A. G. Maki, *ibid.* 11, 62 (1967).
[169]A. G. Maki, *ibid.* 12, 122 (1968).
[170]R. G. Jones, C. C. Bradley, J. Chamberlain, H. A. Gebbie, N. W. B. Stone, and H. Sixsmith, Appl. Opt. 8, 701 (1969).
[171]A. Crocker, H. A. Gebbie, M. F. Kimmitt, and L. E. S. Mathias, Nature 201, 250 (1964).
[172]L. E. S. Mathias and A. Crocker, Phys. Lett. 13, 35 (1964).
[173]D. P. Akitt, W. Q. Jeffers, and P. D. Coleman, Proc. IEEE 54, 547 (1966).
[174]W. Q. Jeffers and P. D. Coleman, Appl. Phys. Lett. 10, 7 (1967).
[175]W. Q. Jeffers and P. D. Coleman, TIIER 55, 168 (1967) [Proc. IEEE 55, 2163 (Dec. 1967)].
[176]W. Q. Jeffers, Appl. Phys. Lett. 11, 178 (1967).
[177]T. Kauya, A. Minoh, and K. Shimoda, J. Phys. Soc. Jpn. 25, 1201 (1968).
[178]G. Kido and N. Miura, Appl. Phys. Lett. 33, 321 (1978).
[179]W. M. Muller and G. T. Flesher, *ibid.* 8, 217 (1966).
[180]M. A. Pollack, T. J. Bridges, and W. J. Tomlinson, *ibid.* 10, 253 (1967).
[181]W. S. Benedict, M. A. Pollack, and W. J. Tomlinson, IEEE J. Quantum Electron. QE-5, 108 (1969).
[182]P. D. Coleman, W. Q. Jeffers, C. Johnson and C. Wittig, IEEE Trans. Electron Devices ED-15, 413 (1968).
[183]R. A. McFarlane and L. H. Fretz, Appl. Phys. Lett. 14, 385 (1969).
[184]O. R. Wood, E. G. Burkhard, M. A. Pollack, and T. J. Bridges, *ibid.* 18, 261 (1971).
[185]P. D. Coleman, IEEE J. Quantum Electron. QE-9, 130 (1973).
[186]B. Adam and F. Kneubühl, J. Appl. Phys. 8, 281 (1975).
[187]C. Sturzenegger, H. Vetsch, and F. Kneubühl, Infrared Phys. 19, 277 (1979).
[188]L. E. S. Mathias, A. Crocker, and M. S. Wills, Phys. Lett. 14, 33 (1965).
[189]D. P. Akitt and C. F. Wittig, J. Appl. Phys. 40, 902 (1969).
[190]D. R. Lide Jr., Phys. Lett. A 24, 599 (1967).
[191]S. F. Dyubko, V. A. Svich, and R. K. Valitov, Pis'ma Zh. Eksp. Teor. Fiz. 7, 408 (1968) [JETP Lett. 7, 320 (1968)].
[192]T. M. Hard, Appl. Phys. Lett. 14, 130 (1969).
[193]J. C. Hassler and P. D. Coleman, *ibid.*, p. 135.
[194]G. Hubner, J. C. Hassler, and P. D. Coleman, *ibid.* 18, 511 (1971).
[195]D. P. Akitt and J. J. Yardley, IEEE J. Quantum Electron. QE-6, 113 (1970).
[196]G. D. Myl'nikov, D. N. Sobolenko, and Yu. V. Shcheblykin, Dokl. Akad. Nauk SSSR 240, 1336 (1978) [Sov. Phys. Doklady 23, 416 (1978)].
[197]Spectroscopic Techniques for the Far-Infrared Submillimeter and Millimeter Spectral Ranges [Russian translation], ed. by T. M. Lifshits, Mir, M., 1970.
[198]Tekhnika submillimetrovykh voln (Submillimeter-Wave Techniques) [in Russian], ed. by R. A. Valitov, Sovetskoe Radio, M., 1969.
[199]Long-Wave Infrared Spectroscopy [Russian translation], ed. by V. N. Murzin, Mir, M., 1966.
[200]F. M. Lussier, Laser Focus, October, 1976, p. 66.

[201]V. D. Bakhtin and G. G. Polovnikov, Prib. Tekh. Eksp. No. 5, 167, 1973.
[202]M. F. Kimmit, Infrared Phys. 18, 675 (1978).
[203]L. S. Kremenchugskiĭ and O. V. Roitsina, Prib. Tekh. Eksp. 3, 7 (1976).
[204]A. Handi, Infrared Phys. 18, 1978.
[205]E. H. Putley, *ibid.*, p. 371.
[206]H. R. Fetterman, B. J. Clifton, P. E. Tannenwald, and C. D. Parker, Appl. Phys. Lett. 24, 70 (1974).
[207]Z. Drozdowicz, P. Woskoboinikow, *et al.*, IEEE J. Quantum Electron. QE-13, 413 (1977).
[208]P. Woskoboinikow *et al.*, Appl. Phys. Lett. 32, 527 (1978).
[209]Z. Drozdowicz, B. Lax, and R. J. Temkin *ibid.* 33, 154 (1978).
[210]P. Woskoboinikow, H. C. Praddaude, W. J. Mulligan, D. R. Cohn, and B. Lax, J. Appl. Phys. 50, 1125 (1979).
[211]H. R. Fetterman, P. E. Tannenwald, C. D. Parker, J. Melngailis, R. C. Williamson, P. Woskoboinikow, H. C. Praddaude, and W. J. Mulligan, Appl. Phys. Lett. 34, 123 (1979).
[212]T. J. Bridges and V. T. Nguyen, *ibid.* 23, 107 (1973).
[213]N. Brignall, R. A. Wood, C. R. Pidgeon, and B. S. Wherrett, Opt. Commun. 12, 17 (1974).
[214]V. T. Nguyen and T. J. Bridges, Publication cited in Ref. 36, p. 139.
[215]D. N. Klyshko, Fotony i nelineĭnaya optika (Photons and Non-linear Optics) [in Russian], Nauka, M., 1980.
[216]H. Park, Bull. Am. Phys. Soc. 25, 891 (1980).
[217]Laser Focus 17, 18 (1980).
[218]*ibid.*, p. 88.
[219]V. S. Letokhov, Usp. Fiz. Nauk 125, 57 (1978) [Sov. Phys. Usp. 21, 405 (1978)].
[220]R. V. Ambartsumyan, Yu. A. Gorokhov, V. S. Letokhov, and G. N. Makarov, Pis'ma Zh. Eksp. Teor. Fiz. 21, 35 (1975) [JETP Lett. 21, 171 (1975)].
[221]R. V. Ambartsumyan, Yu. A. Gorokhov, V. S. Letokhov, and G. N. Makarov, *ibid.* 22, 96 (1975) [JETP Lett. 22, 43 (1975)].
[222]V. G. Averin, A. N. Babichev, G. S. Baronov, M. G. Karchevskiĭ, N. S. Krasnikov, A. Yu. Kulikov, A. V. Merzlyakov, M. G. Morozov, A. I. Pisanko, and E. P. Skvortsova, Kvantovaya Elektron. (Moscow) 6, 2637 (1979) [Sov. J. Quantum Electron. 9, 1565 (1979)].
[223]B. I. Vasil'ev, A. P. Dyad'kin, A. N. Sukhanov, Pis'ma Zh. Tekh. Fiz. 6, 311 (1980) [Sov. Tech. Phys. Lett. 6, 135 (1980)].
[224]P. Rabinowitz, A. Stein, R. Brickman, and A. Kaldor, Appl. Phys. Lett. 35, 739 (1979).
[225]N. Bloembergen, Usp. Fiz. Nauk 97, 307 (1969) [Amer. J. Phys. 35(11), 989 (1967)].
[226]P. P. Sorokin and J. R. Lankard, IEEE J. Quantum Electron. QE-9, 227 (1973).
[227]F. De Martini, J. Appl. Phys. 37, 4503 (1966).
[228]B. A. Akanaev, S. A. Akhmanov, and Yu. G. Khronopulo, Zh. Eksp. Teor. Fiz. 55, 1253 (1968) [Sov. Phys. JETP 28, 656 (1969)].
[229]M. G. Mayer, C. R. Acad. Sci. Ser. B 266, 123 (1968).
[230]V. S. Butylkin, D. Yu. Kozyarskiĭ, E. N. Plyusnina, P. S. Fisher, and Yu. G. Khronopulo, Kvantovaya Elektron. (Moscow) 2, 2282 (1975) [Sov. J. Quantum Electron. 5, 1242 (1975)].
[231]R. W. F. Gross, Opt. Eng. 13, 506 (1974).
[232]V. S. Butylkin, A. E. Kaplan, Yu. G. Khronopulo, and E. I. Yakubovich, Rezonansnye vzaimodeĭstviya sveta s veshchestvom (Resonance Interaction of Light with Matter) [in Russian], Nauka, M., 1977.
[233]C. K. N. Patel and E. D. Shaw, Phys. Rev. B 3, 1279 (1971).
[234]Yu. I. Buchkov, E. K. Karlova, and N. V. Karlov, Pis'ma Zh. Tekh. Fiz. 2, 212 (1976) [Sov. Tech. Phys. Lett. 2, 81 (1976)].

Translated by S. Chomet